Systematic study of α decay half-lives within the Generalized Liquid Drop Model with various versions of proximity energies*

Jun-Gang Deng(邓军刚)[1] Hong-Fei Zhang(张鸿飞)[1,2,3†]

[1]School of Nuclear Science and Technology, Lanzhou University, 730000 Lanzhou, China
[2]Joint Department for Nuclear Physics, Institute of Modern Physics, CAS and Lanzhou University, 730000 Lanzhou, China
[3]Engineering Research Center for Neutron Application, Ministry of Education, Lanzhou University, 730000 Lanzhou, China

Abstract: It is universally acknowledged that the Generalized Liquid Drop Model (GLDM) has two advantages over other α decay theoretical models: introduction of the quasimolecular shape mechanism and proximity energy. In the past few decades, the original proximity energy has been improved by numerous works. In the present work, the different improvements of proximity energy are examined when they are applied to the GLDM for enhancing the calculation accuracy and prediction ability of α decay half-lives for known and unsynthesized superheavy nuclei. The calculations of α half-lives have systematic improvements in reproducing experimental data after choosing a more suitable proximity energy for application to the GLDM. Encouraged by this, the α decay half-lives of even-even superheavy nuclei with Z=112-122 are predicted by the GLDM with a more suitable proximity energy. The predictions are consistent with calculations by the improved Royer formula and the universal decay law. In addition, the features of the predicted α decay half-lives imply that the next double magic nucleus after ^{208}Pb is ^{298}Fl.

Keywords: α decay, superheavy nuclei, Generalized Liquid Drop Model, proximity energy

DOI: 10.1088/1674-1137/abcc5a

I. INTRODUCTION

α decay, one of the most important decay modes of heavy and superheavy nuclei, attracts constant attention [1-4] because it can be a probe to reveal some important nuclear structure information, such as the properties of the ground state, nuclear deformation, nuclear shape coexistence, energy levels, and so on [5-13], and can be an important tool to identify the new synthesized superheavy nuclei [14-21].

Constructing a reasonable nuclear potential between an α-particle and a daughter nucleus is the most crucial issue in many α decay theoretical models, because the α decay half-life is mainly determined by the barrier penetrating probability [22]. There are many α decay models choosing different nuclear potentials between the α-particle and the daughter nucleus, such as the Coulomb and proximity potential model with proximity potential [23-26], the two-potential approach with a cosh parametrized form nuclear potential [27-29], the density-dependent cluster model with a double-folding integral of the renormalized M3Y nucleon-nucleon potential [30-34], the preformed cluster model with SLy4 Skyrme-like effective interaction [9, 35, 36], and so on.

Unlike other models, the Generalized Liquid Drop Model (GLDM) has two major advantages: introducing the quasimolecular shape mechanism [37], which can describe the complex deformation process from the parent nucleus continuous transition to the appearance of a deep and narrow neck, finally resulting in two tangential fragments, and adding the proximity energy, including an accurate radius and mass asymmetry. When a neck or a gap appears in one-body shapes or between separated fragments, proximity energy plays a key role in taking into account the effects of the nuclear forces between the close surfaces, balancing the repulsion of the Coulomb barrier, and reasonably constructing the barrier heights and positions of the nucleus in complex deformation processes [37-40]. Therefore, the GLDM can successfully deal with proton radioactivity [41], cluster radioactivity [42], fusion [43], fission [44] and the α decay process [22, 37, 40, 45-48].

The proximity energy was first proposed by Blocki *et al*. [49] for describing the interaction energy associated with the crevice or neck in the nuclear configuration that would be expected immediately after contact of two nuc-

Received 30 July 2020; Accepted 15 October 2020; Published online 16 December 2020

* Support by National Natural Science Foundation of China (10775061, 11175054, 11675066, 11665019, 11947229), the Fundamental Research Funds for the Central Universities (lzujbky-2017-ot04, lzujbky-2020-it01), and Feitian Scholar Project of Gansu province

† E-mail: zhanghongfei@lzu.edu.cn

lei in heavy-ion reactions. Therefore, it was also introduced into the GLDM by Royer [37] to take account of the effects of the nucleon–nucleon force inside the neck or the gap between the nascent or separated α-particle and daughter nucleus. The proximity energies are also used to study the fusion reaction cross sections and nuclear decay (including proton radioactivity, α decay, and cluster radioactivity), because these decay modes proceed in the opposite direction of fusion between a particle or cluster and the daughter nucleus [50, 51]. The proximity energy is based on the proximity force theorem [49, 52], which is described as the product of a factor depending on the mean curvature of the interaction surface and a universal function (depending on the separation distance) and is independent of the masses of colliding nuclei [53, 54]. In the past few decades, numerous works have been devoted to improving the original proximity energy (Prox. 77) [49], by either adopting a better form of the surface energy coefficients [55-62] or introducing an improved universal function or another nuclear radius parameterization [52, 53, 63-74].

In order to obtain more precise calculations of α decay half-lives for known nuclei and to enhance the prediction ability of α decay half-lives and the island of stability for superheavy nuclei, it is very important and interesting to develop the GLDM by adopting a more suitable proximity energy for constructing a reasonable potential barrier based on available α decay experimental data. This is the purpose of the present work. We also notice that there have been some works using the GLDM with proximity energy Prox. 81 [52] or proximity energy Denisov [73] instead of the original proximity energy formalism in the GLDM to study the α decay [75-78]. The calculations can reproduce the experimental data better than those calculated by the original GLDM. However, in the present work, we find that proximity energy Prox. 81 [52] is not the most suitable substitute for the original one, and the proximity energy Denisov [73] has a different nuclear radius formalism from that of the GLDM, which is not self-consistent for calculation. In this work, for self-consistency, we choose 16 various versions of proximity energies that have the same radii forms as the GLDM and systematically study the applicability of these when applied to the GLDM. The calculations indicate that GLDM with the proximity energy Prox. 77-Set 13 gives the lowest root-mean-square (RMS) deviation in reproducing experimental α half-lives. Using GLDM with proximity energy Prox. 77-Set 13, we predict α decay half-lives of superheavy even-even nuclei with $Z = 112-122$. The predictions are compared with the ones calculated by the improved Royer formula [79] and the universal decay law (UDL) [80].

This article is organized as follows. In Sec. II, theoretical framework for the α decay half-life and the GLDM are briefly presented. The detailed calculations and discussion are given in Sec. III. Sec. IV presents a brief summary.

II. THEORETICAL FRAMEWORK

A. The generalized liquid drop model

The α decay half-life can be calculated with decay constant λ as

$$T_{1/2} = \frac{\ln 2}{\lambda}. \tag{1}$$

In the framework of the GLDM [22, 37, 40, 45-48], the α decay constant λ can be obtained by the product of α-particle preformation factor P_α, the assault frequency ν, and the barrier penetrating probability P:

$$\lambda = P_\alpha \nu P. \tag{2}$$

The α-particle preformation factor P_α can be estimated by the analytic formula put forwarded in our previous work [81]. It is expressed as

$$\log_{10} P_\alpha = a + bA^{1/6}\sqrt{Z} + c\frac{Z}{\sqrt{Q_\alpha}} - d\chi' - e\rho' + f\sqrt{l(l+1)}, \tag{3}$$

where $\chi' = Z_1 Z_2 \sqrt{\frac{A_1 A_2}{(A_1+A_2)Q_\alpha}}$ and $\rho' = \sqrt{\frac{A_1 A_2}{A_1+A_2} Z_1 Z_2 (A_1^{1/3}+A_2^{1/3})}$; A, Z represent the mass number and proton number of the α decay parent nucleus, respectively; l is the angular momentum taken away by the α-particle; and the values of adjustable parameters a, b, c, d, e, and f are fitted by the extracted α-particle preformation factor from the ratios of calculated α decay half-lives with $P_\alpha = 1$ to experimental data and are listed in Table 3.

The assault frequency ν can be obtained by

$$\nu = \frac{1}{2R_0}\sqrt{\frac{2E_\alpha}{M}}, \tag{4}$$

with E_α and M_α being the kinetic energy and mass of the α-particle, respectively; R_0 is the radius of the α decay parent nucleus obtained by

$$R_i = 1.28A_i^{1/3} - 0.76 + 0.8A_i^{-1/3} (i = 0, 1, 2). \tag{5}$$

The barrier penetrating probability P can be obtained by Wentzel-Kramers-Brillouin (WKB) approximation as

$$P = \exp\left[-\frac{2}{\hbar}\int_{r_{\rm in}}^{r_{\rm out}} \sqrt{2B(r)(E_r - E(\text{sphere}))}\,\mathrm{d}r\right], \tag{6}$$

where r represents the center of mass distance between

the preformed α-particle and the daughter nucleus. The classical turning points $r_{\rm in}$ and $r_{\rm out}$ can be obtained by $r_{\rm in} = R_1 + R_2$ and $E(r_{\rm out}) = Q_\alpha$. $B(r) = \mu$ represents the reduced mass between the preformed α-particle and daughter nucleus.

The total interaction potential E in the GLDM is composed of five parts [37]: volume energy $E_{\rm V}$, surface energy $E_{\rm S}$, Coulomb energy $E_{\rm C}$, proximity energy $E_{\rm Prox}$, and centrifugal potential E_l.

$$E = E_{\rm V} + E_{\rm S} + E_{\rm C} + E_{\rm Prox} + E_l. \tag{7}$$

For one-body shapes, the volume, surface, and Coulomb energies are expressed as

$$E_{\rm V} = -15.494(1 - 1.8I^2)A, \tag{8}$$

$$E_{\rm S} = 17.9439(1 - 2.6I^2)A^{2/3}(S/4\pi R_0^2), \tag{9}$$

$$E_{\rm C} = 0.6e^2(Z^2/R_0)\times 0.5\int (V(\theta)/V_0)(R(\theta)/R_0)^3 \sin\theta {\rm d}\theta, \tag{10}$$

where S denotes the surface of the one-body deformed nucleus, I is the relative neutron excess, $V(\theta)$ represents the electrostatic potential at the surface, and V_0 is the surface potential of the sphere.

For two separated fragments, the volume, surface, and Coulomb energies are defined as

$$E_{\rm V} = -15.494[(1 - 1.8I_1^2)A_1 + (1 - 1.8I_2^2)A_2], \tag{11}$$

$$E_{\rm S} = 17.9439[(1 - 2.6I_1^2)A_1^{2/3} + (1 - 2.6I_2^2)A_2^{2/3}], \tag{12}$$

$$E_{\rm C} = 0.6e^2Z_1^2/R_1 + 0.6e^2Z_2^2/R_2 + e^2Z_1Z_2/r, \tag{13}$$

with A_i, Z_i, R_i, and I_i being the mass numbers, proton numbers, radii, and the relative neutron excesses of the α-particle and the daughter nucleus, respectively.

The centrifugal barrier $E_l(r)$ can be calculated by

$$E_l(r) = \frac{\hbar^2 l(l+1)}{2\mu r^2}. \tag{14}$$

On the basis of the conservation laws of angular momentum and parity [82], the minimum angular momentum $l_{\rm min}$ carried by an α-particle can be obtained by

$$l_{\rm min} = \begin{cases} \Delta_j, & \text{for even } \Delta_j \text{ and } \pi_p = \pi_d, \\ \Delta_j + 1, & \text{for even } \Delta_j \text{ and } \pi_p \neq \pi_d, \\ \Delta_j, & \text{for odd } \Delta_j \text{ and } \pi_p \neq \pi_d, \\ \Delta_j + 1, & \text{for odd } \Delta_j \text{ and } \pi_p = \pi_d, \end{cases} \tag{15}$$

where $\Delta_j = |j_p - j_d|$, j_p, π_p, j_d, π_d are the spin and parity values of the parent and daughter nuclei, respectively.

B. The proximity energy

The surface energy comes from the effects of the surface tension forces in half-space. When a neck or a gap appears in one-body shapes or between separated fragments, an additional term called the proximity energy must be added to take into account the effects of the nuclear forces between the close surfaces [37, 40]. The proximity energy is described as the product of a factor depending on the mean curvature of the interaction surface and a universal function depending on the separation distance [53, 54].

In the present work, for self-consistency, we choose 16 various versions of proximity energies that have the same radii forms as the GLDM, including proximity energy formalisms Prox. 77 [49] and its 12 modified forms on the basis of improving the surface energy coefficients [55-62], Bass 80 [69], Prox. 81 [52], and Guo 2013 [74]. Proximity energy Prox. 77 [49] and its 12 modified forms are expressed as

$$E_{\rm Prox}(r) = 4\pi\gamma b\bar{R}\phi(\xi), \tag{16}$$

where the mean curvature radius $\bar{R}$ can be obtained as

$$\bar{R} = \frac{C_1C_2}{C_1 + C_2}, \tag{17}$$

where C_1 and C_2 denote the matter radii of the α-particle and the daughter nucleus, respectively, which are given by

$$C_i = R_i\left[1 - (\frac{b}{R_i})^2\right](i = 1, 2), \tag{18}$$

with the effective sharp radius R_i obtained by Eq. (5).

The surface energy coefficient γ can be obtained by

$$\gamma = \gamma_0(1 - k_sA_s^2), \tag{19}$$

where $A_s = \dfrac{N-Z}{N+Z}$ represents neutron-proton excess. The surface energy constant γ_0 and the surface asymmetry constant k_s are set in various improvements as

Set 1: $\gamma_0 = 0.9517$ (MeV/fm^2), $k_s = 1.7826$ [49],
Set 2: $\gamma_0 = 1.01734$ (MeV/fm^2), $k_s = 1.79$ [55],
Set 3: $\gamma_0 = 1.460734$ (MeV/fm^2), $k_s = 4.0$ [56],
Set 4: $\gamma_0 = 1.2402$ (MeV/fm^2), $k_s = 3.0$ [57],
Set 5: $\gamma_0 = 1.1756$ (MeV/fm^2), $k_s = 2.2$ [58],
Set 6: $\gamma_0 = 1.27326$ (MeV/fm^2), $k_s = 2.5$ [58],
Set 7: $\gamma_0 = 1.2502$ (MeV/fm^2), $k_s = 2.4$ [58],
Set 8: $\gamma_0 = 0.9517$ (MeV/fm^2), $k_s = 2.6$ [59],

Set 9: $\gamma_0 = 1.2496$ (MeV/fm^2), $k_s = 2.3$ [60],
Set 10: $\gamma_0 = 1.25284$ (Mev/fm^2), $k_s = 2.345$ [61],
Set 11: $\gamma_0 = 1.08948$ (MeV/fm^2), $k_s = 1.9830$ [62],
Set 12: $\gamma_0 = 0.9180$ (MeV/fm^2), $k_s = 0.7546$ [62],
Set 13: $\gamma_0 = 0.911445$ (MeV/fm^2), $k_s = 2.2938$ [62].
The universal function $\phi(\xi)$ is expressed as

$$\phi(\xi) = \begin{cases} -\frac{1}{2}(\xi-\xi_0)^2 - 0.0852(\xi-\xi_0)^3, & 0 < \xi \leqslant 1.2511, \\ -3.347\exp\left(\frac{-\xi}{0.75}\right), & \xi \geqslant 1.2511, \end{cases} \tag{20}$$

where $\xi_0 = 2.54$. $\xi = \frac{r - C_1 - C_2}{b}$ is the distance between the near surface of the α-particle and daughter nucleus with the width parameter b taken as unity.

III. RESULTS AND DISCUSSION

The aim of the present work is to develop the GLDM for enhancing calculation accuracy and prediction ability of α decay half-lives for known and unsynthesized superheavy nuclei by chosing a more suitable proximity energy in constructing a reasonable potential barrier.

If the improved versions of the original proximity energy can be applied to the GLDM, three conditions need to be met: first, the radii formulas for the proximity energy and GLDM should be the same; second, the total GLDM energy, including the proximity energy, between the α-particle and daughter nucleus should be reasonable; and finally, the calculated α decay half-lives by the GLDM with the best selected proximity energy should give the lowest RMS deviation in reproducing experimental α half-lives. Therefore, we comparatively study the abilities of 16 various versions of proximity energies when they are applied to the GLDM for describing the α decay half-lives, in which the proximity energies have the same radii forms as the GLDM. These proximity energies include Prox. 77 [49] and its 12 modified forms on the basis of improving the surface energy coefficients [55-62], Bass 80 [69], Prox. 81 [52], and Guo 2013 [74].

In these various versions of proximity energies, we find that the proximity energy Guo 2013 [74] is not suitable for application to the GLDM because for some α decay nuclei such as ^{148}Gd, the total nuclear potential distribution shows short-term decline, even less than zero, after the two tangent fragments have separated, which results from the proximity energy determining too strong an attractive interaction potential.

For choosing the most suitable one from the remainder of proximity energies that can be applied to the GLDM, we calculate the RMS deviation between the calculated α decay half-lives by the GLDM with various proximity energies, where the α-particle preformation factor is assumed as the constant $P_\alpha = 1$, and experimental data for all 535 nuclei, including 159 even-even nuclei, 295 odd-A nuclei, and 81 doubly odd nuclei using

$$\sigma = \sqrt{\frac{1}{n}\sum\left(\log_{10}T_{1/2}^{\rm cal} - \log_{10}T_{1/2}^{\rm exp}\right)^2}. \tag{21}$$

The results are listed in Table 1. In this table, we can find that the σ values are all greater than 1, indicating that there are average deviations of more than one order of magnitude between the calculations and the experimental data because α-particle preformation factors are assumed as $P_\alpha = 1$, which are overestimated. In addition, we find that the values of σ are different when caused by the GLDM with various proximity energies. The minimum $\sigma = 1.459$ and maximum $\sigma = 1.644$ are caused by the GLDM with proximity energies Prox. 77-Set 13 and Bass 80, respectively.

The experimental data and calculations of α decay half-lives for ^{148}Gd, as an example, are listed in Table 2. From this table, one can find that the GLDM with various proximity energies calculates different α decay half-lives. Further, all calculations are an order of magnitude smaller than the experimental data, indicating that the α-

Table 1. The RMS deviations between calculated α decay half-lives by GLDM with different versions of proximity energies and experimental data.

GLDM with proximity energy	σ	GLDM with proximity energy	σ
Prox. 77-Set 1	1.472	Prox. 77-Set 2	1.488
Prox. 77-Set 3	1.579	Prox. 77-Set 4	1.534
Prox. 77-Set 5	1.525	Prox. 77-Set 6	1.546
Prox. 77-Set 7	1.541	Prox. 77-Set 8	1.467
Prox. 77-Set 9	1.542	Prox. 77-Set 10	1.543
Prox. 77-Set 11	1.505	Prox. 77-Set 12	1.471
Prox. 77-Set 13	1.459	Bass 80	1.644
Prox. 81	1.500	original one	1.605

Table 2. The α decay half-lives of calculations by GLDM with different versions of proximity energies and experimental data for ^{148}Gd.

method	α decay half-lives for ^{148}Gd/s
experimental data	2.24×10^{9}
GLDM with original proximity energy	4.83×10^{8}
GLDM with Prox. 77- Set 1	6.93×10^{8}
GLDM with Prox. 77- Set 2	6.49×10^{8}
GLDM with Prox. 77- Set 3	4.31×10^{8}
GLDM with Prox. 77- Set 4	5.30×10^{8}
GLDM with Prox. 77- Set 5	5.56×10^{8}
GLDM with Prox. 77- Set 6	5.05×10^{8}
GLDM with Prox. 77- Set 7	5.16×10^{8}
GLDM with Prox. 77- Set 8	7.03×10^{8}
GLDM with Prox. 77- Set 9	5.15×10^{8}
GLDM with Prox. 77- Set 10	5.14×10^{8}
GLDM with Prox. 77- Set 11	6.05×10^{8}
GLDM with Prox. 77- Set 12	7.04×10^{8}
GLDM with Prox. 77- Set 13	7.28×10^{8}
GLDM with Bass 80	3.90×10^{8}
GLDM with Prox. 81	6.33×10^{8}

particle preformation factor is on the order of 10^{-1}. In addition, one can see that most of the calculations by the GLDM with improved proximity energies are better than the ones by the original GLDM from the aspect of reproducing experimental data. However, the GLDM with proximity energy Bass 80 gives a worse calculation than the one calculated by the original GLDM, showing that it is not appropriate for application to the GLDM. The calculation by the GLDM with proximity energy Prox. 77-Set 13 gives the closest reproduction of the experimental data. Why are calculations by the GLDM with various proximity energies different from each other? Based on our comparative analysis, we can explore what particular feature of a given potential impacts these differences between various theoretical calculations, as well as differences between theory and experiments. From Sec. II.A, we find that the α decay half-life can be obtained using the α-particle preformation factor, which is assumed as the constant $P_\alpha = 1$ in comparing proximity energies, the assault frequency ν, which is dependent on α decay energy Q_α, and barrier penetration probability P, which is related to the total GLDM energy. However, for an α decay nucleus, Q_α and the assault frequency ν are fixed. Therefore, these have different total GLDM energies, and various versions of the proximity energies cause the differences between calculated α decay half-lives. In order to verify this conclusion, taking ^{148}Gd, for instance, we plot its 16 versions of total GLDM energy distributions, including the original proximity energy and its 15 improved versions, in Fig. 1. In this figure, we can see that the proximity energies only work in the short region from 7.8 to 12 fm. After the α-particle and daughter nuclei are separated, the proximity energies are equal to zero.

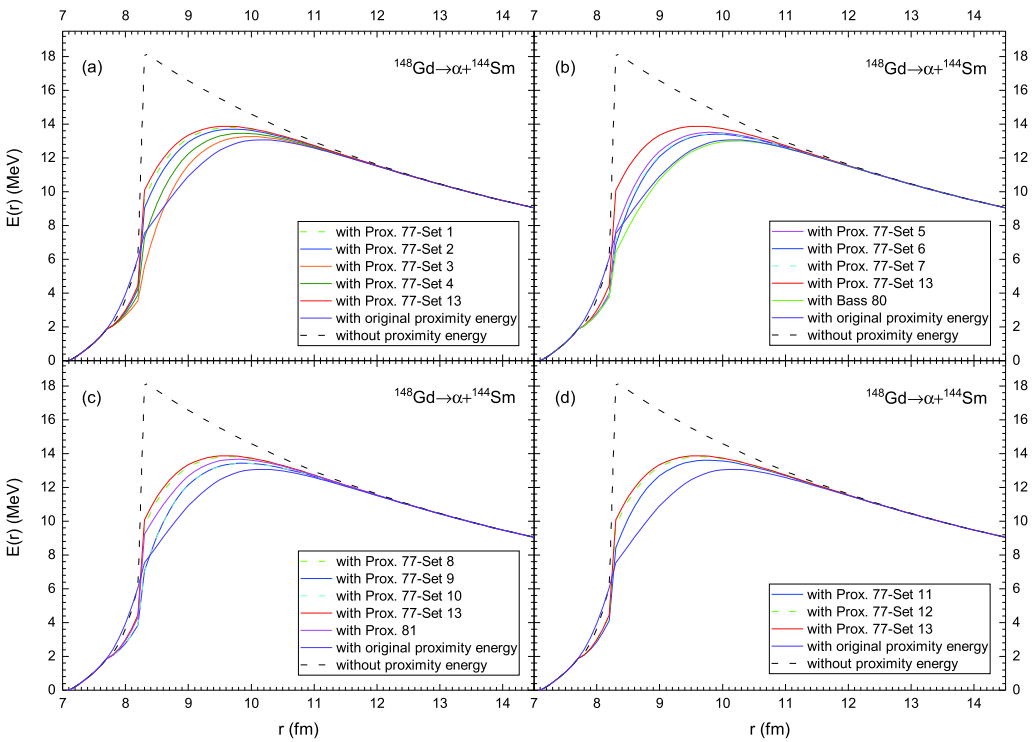

Fig. 1. (color online) The distributions of total GLDM energies including various versions of proximity energies for ^{148}Gd.

Therefore, as can be seen from Section 2.1, the classic turning points $r_{in} = R_1 + R_2$ and $E(r_{out}) = Q_\alpha$ in the GLDM with various proximity energies are the same. In addition, we see that the proximity energies can lower the height of the potential barriers, and their attractive effect balances the Coulomb repulsion between the two fragments. Further, the peaks of potential barriers are shifted toward more external positions. Thus, the different proximity energies cause changes in the shape and height of the total GLDM energy distributions.

The same values of r_{in} and r_{out} as well as the highest height of $E(r)$ in the GLDM with proximity energy Prox. 77-Set 13 result in the minimum barrier penetration probability P. Thus, the calculated α decay half-life is the maximum one in Table 2. Similarly, the lowest height of $E(r)$ in the GLDM with proximity energy Bass 80 resulted in the minimum calculation. It is shown that the proximity energy is very important in the GLDM, because it affects the shape and height of the total potential barrier, which determines the possibility of barrier penetration and in turn leads to the theoretical calculation of α decay half-life. Therefore, it is interesting and important to find the most suitable proximity energy for developing the GLDM to obtain precise calculations and enhance the prediction ability of α decay half-lives. From Tables 1 and 2, it is shown that the proximity energy Prox. 77-Set 13 is the most suitable one for application to the GLDM for describing the α decay half-lives. The σ values indicate that, compared with the original GLDM, the calculated α decay half-lives using the GLDM with proximity energy Prox. 77-Set 13 are improved by $\frac{1.605-1.459}{1.605} = 9.1\%$. Although the relative value is not large, this is a significant improvement on the GLDM because the proximity energy can affect the total interaction potential in a short region.

In our previous work [81], we proposed an analytic formula for estimating the α-particle preformation factor, i.e., Eq. (3). In this work, because we choose a more suitable proximity energy in the GLDM, the parameters of Eq. (3) should be redetermined. First, we extract the α-particle preformation factor using the ratio of the calculated α decay half-life within the GLDM with proximity energy Prox. 77-Set 13 and $P_\alpha = 1$ to the experimental data. We then use the extracted α-particle preformation factor and Eq. (3) to obtain the parameters, which are listed in Table 3.

The calculated α decay half-lives and experimental data are listed in Tables 4-6 for even-even nuclei, odd-A nuclei, and doubly odd nuclei, respectively. In each part of these three tables, the first four columns represent the α decay parent nucleus, the daughter nucleus, experimental α decay energy, and the minimum angular momentum taken away by the α-particle, while the spin and parity values for the α decay parent and daughter nuclei are taken from the latest evaluated nuclear properties table NUBASE2016 [83], respectively. The fifth one represents the experimental α decay half-life. The sixth one represents the calculated α decay half-life within the original GLDM with $P_\alpha = 1$. The seventh one represents the calculated α decay half-life by GLDM with proximity energy Prox. 77-Set 13 and $P_\alpha = 1$. The eighth one represents the obtained α-particle preformation factor from Eq. (3). The last one represents the calculated α decay half-life within the GLDM with proximity energy Prox. 77-Set 13 and estimated α-particle preformation factor from Eq. (3). From these three tables, it is seen that, compared with $\lg T_{1/2}^{\rm cal1}$, $\lg T_{1/2}^{\rm cal2}$ has a significant improvement in conformity with the experimental data. However, both $\lg T_{1/2}^{\rm cal1}$ and $\lg T_{1/2}^{\rm cal2}$ are smaller than experimental data by more than an order of magnitude on the whole. This is because the α preformation factor is assumed as $P_\alpha = 1$, which is overestimated. Therefore, an α preformation factor P_α should be introduced in the theoretical model. After considering the α-particle preformation factor calculated by Eq. (3), $\lg T_{1/2}^{\rm cal3}$ can well reproduce the experimental data.

The differences between logarithmic values of the three calculated α decay half-lives and the experimental data are denoted as black open squares, red solid squares, and blue solid circles in Figs. 2-4 for even-even nuclei, odd-A nuclei and doubly odd nuclei, respectively. From these figures, it is seen that $\lg T_{1/2}^{\rm cal1}$ is significantly less than the experimental value. After adopting the GLDM with proximity energy Prox. 77-Set 13, compared with $\lg T_{1/2}^{\rm cal1}$, $\lg T_{1/2}^{\rm cal2}$ is significantly improved in reproducing the experimental data. In addition, when the neutron

Table 3. The parameters of Eq. (3) for estimating the α-particle preformation factor.

nuclei	region	a	b	c	d	e	f
even-even nuclei	$N \le 126$	−9.4985	−8.9005	4.0450	1.0432	−2.9731	−
	$N > 126$	−2.1047	0.1230	4.2051	1.0681	0.0533	−
odd-A nuclei	$N \le 126$	−24.5445	−13.2233	9.9493	2.5690	−4.5754	−0.0350
	$N > 126$	1.3626	−6.2523	−0.0252	−0.0155	−1.9616	−0.0937
doubly odd nuclei	$N \le 126$	−2.7484	−4.2572	2.2748	0.5947	−1.3917	−0.0901
	$N > 126$	−37.5320	−20.0571	23.5391	6.0638	−6.9409	−0.2030

Table 4. Calculations of α decay half-lives for even-even nuclei. Experimental α decay half-lives are taken from the latest evaluated nuclear properties table NUBASE2016 [83]. The α decay energies are taken from the latest evaluated atomic mass table AME2016 [84, 85]. The α decay energies and half-lives are in units of MeV and s, respectively.

α transition		Q_α	$l_{\min}$	$\lg T_{1/2}^{\rm exp}$	$\lg T_{1/2}^{\rm cal1}$	$\lg T_{1/2}^{\rm cal2}$	P_α	$\lg T_{1/2}^{\rm cal3}$
^{148}Gd	^{144}Sm	3.27	0	9.35	8.68	8.86	0.2841	9.41
^{150}Dy	^{146}Gd	4.35	0	3.07	2.17	2.21	0.1775	2.96
^{154}Dy	^{150}Gd	2.95	0	13.98	13.17	13.39	0.3075	13.9
^{154}Er	^{150}Dy	4.28	0	4.68	3.72	3.95	0.1845	4.69
^{154}Yb	^{150}Er	5.47	0	−0.35	−1.39	−1.15	0.1601	−0.36
^{158}Yb	^{154}Er	4.17	0	6.63	5.52	5.55	0.1917	6.27
^{158}Hf	^{154}Yb	5.41	0	0.35	−0.18	−0.15	0.165	0.64
^{162}Hf	^{158}Yb	4.42	0	5.69	5.07	5.2	0.1719	5.96
^{160}W	^{156}Hf	6.07	0	−0.99	−2.05	−1.91	0.1616	−1.12
^{164}W	^{160}Hf	5.28	0	2.22	1.31	1.52	0.1501	2.34
^{168}W	^{164}Hf	4.5	0	6.2	5.57	5.71	0.1439	6.55
^{162}Os	^{158}W	6.77	0	−2.68	−3.76	−3.58	0.1623	−2.79
^{168}Os	^{164}W	5.82	0	0.68	−0.23	−0.08	0.1327	0.79
^{172}Os	^{168}W	5.22	0	3.23	2.46	2.54	0.1171	3.48
^{186}Os	^{182}W	2.82	0	22.8	21.72	21.89	0.1048	22.87
^{168}Pt	^{164}Os	6.99	0	−2.69	−3.78	−3.65	0.14	−2.8
^{174}Pt	^{170}Os	6.18	0	0.06	−0.95	−0.76	0.1096	0.2
^{178}Pt	^{174}Os	5.57	0	2.43	1.63	1.71	0.0953	2.73
^{182}Pt	^{178}Os	4.95	0	5.62	4.83	5.02	0.0842	6.09
^{190}Pt	^{186}Os	3.27	0	19.31	17.86	17.98	0.0797	19.08
^{174}Hg	^{170}Pt	7.23	0	−2.7	−3.9	−3.7	0.1206	−2.78
^{178}Hg	^{174}Pt	6.58	0	−0.53	−1.69	−1.59	0.1029	−0.6
^{182}Hg	^{178}Pt	6	0	1.89	0.62	0.81	0.0876	1.87
^{186}Hg	^{182}Pt	5.2	0	5.7	4.37	4.55	0.0778	5.66
^{180}Pb	^{176}Hg	7.42	0	−2.39	−3.81	−3.62	0.1049	−2.64
^{186}Pb	^{182}Hg	6.47	0	1.07	−0.54	−0.36	0.0813	0.73
^{190}Pb	^{186}Hg	5.7	0	4.24	2.81	2.93	0.0703	4.08
^{186}Po	^{182}Pb	8.5	0	−4.47	−6.36	−6.16	0.086	−5.09
^{194}Po	^{190}Pb	6.99	0	−0.41	−1.79	−1.6	0.0608	−0.38
^{198}Po	^{194}Pb	6.31	0	2.27	0.82	1	0.0512	2.29
^{202}Po	^{198}Pb	5.7	0	5.14	3.53	3.64	0.0431	5.01
^{206}Po	^{202}Pb	5.33	0	7.14	5.44	5.61	0.0357	7.06
^{212}Po	^{208}Pb	8.95	0	−6.53	−8	−7.81	0.1047	−6.83
^{216}Po	^{212}Pb	6.91	0	−0.84	−1.86	−1.69	0.1921	−0.97
^{194}Rn	^{190}Po	7.86	0	−3.11	−3.9	−3.72	0.0708	−2.57
^{200}Rn	^{196}Po	7.04	0	0.07	−1.22	−1.04	0.053	0.23
^{204}Rn	^{200}Po	6.55	0	2.01	0.61	0.78	0.0438	2.14
^{208}Rn	^{204}Po	6.26	0	3.37	1.79	1.91	0.0358	3.35
^{212}Rn	^{208}Po	6.38	0	3.16	1.15	1.31	0.0287	2.86
^{150}Gd	^{146}Sm	2.81	0	13.75	13.17	13.17	0.3578	13.62
^{152}Dy	^{148}Gd	3.73	0	6.93	6.26	6.32	0.2117	6.99
^{152}Er	^{148}Dy	4.94	0	1.06	0.12	0.26	0.1635	1.05
^{156}Er	^{152}Dy	3.48	0	10.24	9.49	9.61	0.2389	10.23
^{156}Yb	^{152}Er	4.81	0	2.41	1.79	1.95	0.1725	2.71
^{156}Hf	^{152}Yb	6.03	0	−1.63	−2.73	−2.55	0.1609	−1.75
^{160}Hf	^{156}Yb	4.9	0	3.28	2.28	2.38	0.1672	3.15
^{158}W	^{154}Hf	6.62	0	−2.9	−4.04	−3.9	0.1645	−3.12
^{162}W	^{158}Hf	5.68	0	0.42	−0.46	−0.31	0.1549	0.5
^{166}W	^{162}Hf	4.86	0	4.74	3.49	3.58	0.1475	4.41
^{180}W	^{176}Hf	2.52	0	25.75	24.54	24.72	0.1572	25.52
^{166}Os	^{162}W	6.14	0	−0.53	−1.55	−1.43	0.1412	−0.58
^{170}Os	^{166}W	5.54	0	1.89	1.01	1.21	0.124	2.12
^{174}Os	^{170}W	4.87	0	5.25	4.35	4.53	0.1122	5.48
^{166}Pt	^{162}Os	7.29	0	−3.52	−4.73	−4.58	0.1518	−3.76
^{172}Pt	^{168}Os	6.46	0	−1	−2.02	−1.9	0.1185	−0.98
^{176}Pt	^{172}Os	5.89	0	1.2	0.28	0.48	0.1019	1.47
^{180}Pt	^{176}Os	5.24	0	4.27	3.28	3.47	0.0898	4.51
^{184}Pt	^{180}Os	4.6	0	7.77	6.94	7.06	0.0803	8.15
^{172}Hg	^{168}Pt	7.53	0	−3.64	−4.79	−4.65	0.1315	−3.77
^{176}Hg	^{172}Pt	6.9	0	−1.65	−2.79	−2.59	0.1114	−1.63
^{180}Hg	^{176}Pt	6.26	0	0.73	−0.47	−0.28	0.0952	0.74
^{184}Hg	^{180}Pt	5.66	0	3.44	2.12	2.23	0.0816	3.32
^{178}Pb	^{174}Hg	7.79	0	−3.64	−4.94	−4.8	0.114	−3.86
^{184}Pb	^{180}Hg	6.77	0	−0.21	−1.64	−1.53	0.0885	−0.48
^{188}Pb	^{184}Hg	6.11	0	2.43	0.94	1.13	0.0752	2.25
^{192}Pb	^{188}Hg	5.22	0	6.55	5.26	5.44	0.0664	6.62
^{190}Po	^{186}Pb	7.69	0	−2.61	−4.08	−3.98	0.0724	−2.84
^{196}Po	^{192}Pb	6.66	0	0.75	−0.58	−0.47	0.0557	0.78
^{200}Po	^{196}Pb	5.98	0	3.79	2.26	2.44	0.047	3.76
^{204}Po	^{200}Pb	5.49	0	6.27	4.61	4.77	0.0393	6.18
^{208}Po	^{204}Pb	5.22	0	7.96	6.06	6.17	0.0323	7.66
^{214}Po	^{210}Pb	7.83	0	−3.79	−4.94	−4.75	0.1419	−3.91
^{218}Po	^{214}Pb	6.12	0	2.27	1.28	1.45	0.2616	2.03
^{196}Rn	^{192}Po	7.62	0	−2.33	−3.16	−3.08	0.0641	−1.89
^{202}Rn	^{198}Po	6.77	0	1.09	−0.27	−0.16	0.0482	1.15
^{206}Rn	^{202}Po	6.38	0	2.74	1.27	1.45	0.0396	2.85
^{210}Rn	^{206}Po	6.16	0	3.95	2.16	2.32	0.0323	3.81
^{214}Rn	^{210}Po	9.21	0	−6.57	−7.97	−7.77	0.0891	−6.72

Continued on next page

Table 4-continued from previous page

α transition		Q_α	$l_{\min}$	$\lg T_{1/2}^{\rm exp}$	$\lg T_{1/2}^{\rm cal1}$	$\lg T_{1/2}^{\rm cal2}$	P_α	$\lg T_{1/2}^{\rm cal3}$
^{216}Rn	^{212}Po	8.2	0	−4.35	−5.3	−5.13	0.1146	−4.19
^{220}Rn	^{216}Po	6.41	0	1.75	0.92	1.09	0.206	1.78
^{202}Ra	^{198}Rn	7.88	0	−2.39	−3.34	−3.24	0.0557	−1.98
^{208}Ra	^{204}Rn	7.27	0	0.1	−1.37	−1.26	0.0412	0.13
^{216}Ra	^{212}Rn	9.53	0	−6.74	−8.08	−7.9	0.075	−6.77
^{220}Ra	^{216}Rn	7.59	0	−1.75	−2.71	−2.54	0.1221	−1.63
^{224}Ra	^{220}Rn	5.79	0	5.5	4.7	4.85	0.2376	5.48
^{208}Th	^{204}Ra	8.2	0	−2.62	−3.65	−3.54	0.0485	−2.22
^{214}Th	^{210}Ra	7.83	0	−1.06	−2.58	−2.41	0.0355	−0.96
^{218}Th	^{214}Ra	9.85	0	−6.93	−8.21	−8.03	0.0634	−6.83
^{222}Th	^{218}Ra	8.13	0	−2.65	−3.69	−3.52	0.0934	−2.5
^{226}Th	^{222}Ra	6.45	0	3.27	2.46	2.62	0.1578	3.42
^{230}Th	^{226}Ra	4.77	0	12.38	11.74	11.89	0.3509	12.34
^{218}U	^{214}Th	8.78	0	−3.26	−4.81	−4.64	0.0344	−3.17
^{224}U	^{220}Th	8.63	0	−3.4	−4.48	−4.31	0.0736	−3.18
^{230}U	^{226}Th	5.99	0	6.24	5.48	5.63	0.1673	6.4
^{234}U	^{230}Th	4.86	0	12.89	12.22	12.37	0.2849	12.91
^{228}Pu	^{224}U	7.94	0	0.32	−1.65	−1.54	0.0785	−0.44
^{232}Pu	^{228}U	6.72	0	4.24	2.98	3.13	0.1114	4.08
^{236}Pu	^{232}U	5.87	0	7.96	6.98	7.12	0.1491	7.95
^{240}Pu	^{236}U	5.26	0	11.32	10.52	10.66	0.1897	11.38
^{244}Pu	^{240}U	4.67	0	15.4	14.6	14.73	0.2508	15.33
^{236}Cm	^{232}Pu	7.07	0	3.35	2.26	2.41	0.0859	3.47
^{240}Cm	^{236}Pu	6.4	0	6.37	5.2	5.35	0.1037	6.33
^{244}Cm	^{240}Pu	5.9	0	8.76	7.7	7.84	0.1204	8.76
^{248}Cm	^{244}Pu	5.16	0	13.08	12.05	12.19	0.1621	12.98
^{240}Cf	^{236}Cm	7.71	0	1.61	0.55	0.7	0.0616	1.91
^{244}Cf	^{240}Cm	7.33	0	3.07	1.96	2.11	0.0657	3.29
^{248}Cf	^{244}Cm	6.36	0	7.46	6.16	6.31	0.0869	7.37
^{252}Cf	^{248}Cm	6.22	0	7.94	6.85	6.99	0.0872	8.05
^{244}Fm	^{240}Cf	8.55	0	−0.11	−1.63	−1.48	0.0434	−0.12
^{252}Fm	^{248}Cf	7.15	0	4.96	3.39	3.53	0.0578	4.77
^{256}Fm	^{252}Cf	7.03	0	5.07	3.83	3.98	0.0573	5.22
^{256}No	^{252}Fm	8.58	0	0.46	−1.18	−1.04	0.0347	0.42
^{256}Rf	^{252}No	8.93	0	0.32	−1.55	−1.4	0.0297	0.13
^{260}Rf	^{256}No	8.9	0	0.02	−1.53	−1.4	0.0286	0.15
^{264}Hs	^{260}Sg	10.59	0	−2.97	−4.97	−4.82	0.0173	−3.06
^{270}Hs	^{266}Sg	9.07	0	0.95	−0.75	−0.62	0.0213	1.05
^{286}Fl	^{282}Cn	10.37	0	−0.46	−2.8	−2.67	0.0115	−0.73
^{290}Lv	^{286}Fl	11.01	0	−2.1	−3.92	−3.79	0.0094	−1.77
^{294}Og	^{290}Lv	11.84	0	−2.94	−5.36	−5.23	0.0076	−3.11
^{218}Rn	^{214}Po	7.26	0	−1.47	−2.37	−2.2	0.1515	−1.38
^{222}Rn	^{218}Po	5.59	0	5.52	4.76	4.91	0.2943	5.44
^{204}Ra	^{200}Rn	7.64	0	−1.22	−2.58	−2.41	0.0504	−1.11
^{214}Ra	^{210}Rn	7.27	0	0.39	−1.49	−1.31	0.03	0.21
^{218}Ra	^{214}Rn	8.55	0	−4.6	−5.61	−5.44	0.094	−4.41
^{222}Ra	^{218}Rn	6.68	0	1.53	0.65	0.81	0.1653	1.59
^{226}Ra	^{222}Rn	4.87	0	10.7	10.04	10.2	0.3838	10.61
^{212}Th	^{208}Ra	7.96	0	−1.5	−2.98	−2.81	0.0394	−1.41
^{216}Th	^{212}Ra	8.07	0	−1.59	−3.41	−3.24	0.0319	−1.75
^{220}Th	^{216}Ra	8.95	0	−5.01	−6.04	−5.86	0.0765	−4.74
^{224}Th	^{220}Ra	7.3	0	0.02	−0.93	−0.76	0.1182	0.16
^{228}Th	^{224}Ra	5.52	0	7.78	7.04	7.15	0.2354	7.77
^{216}U	^{212}Th	8.53	0	−2.16	−4.05	−3.89	0.0382	−2.47
^{222}U	^{218}Th	9.48	0	−5.33	−6.74	−6.57	0.0612	−5.36
^{226}U	^{222}Th	7.7	0	−0.57	−1.56	−1.4	0.0935	−0.37
^{232}U	^{228}Th	5.41	0	9.34	8.64	8.79	0.2148	9.46
^{236}U	^{232}Th	4.57	0	14.87	14.21	14.35	0.3309	14.83
^{230}Pu	^{226}U	7.18	0	2.01	1.08	1.23	0.0971	2.24
^{234}Pu	^{230}U	6.31	0	5.72	4.82	4.97	0.1269	5.87
^{238}Pu	^{234}U	5.59	0	9.44	8.49	8.63	0.1647	9.41
^{242}Pu	^{238}U	4.98	0	13.07	12.3	12.45	0.2137	13.12
^{234}Cm	^{230}Pu	7.37	0	2.28	1.15	1.31	0.08	2.41
^{238}Cm	^{234}Pu	6.67	0	5.31	3.95	4.1	0.0962	5.11
^{242}Cm	^{238}Pu	6.22	0	7.15	6.08	6.23	0.1085	7.19
^{246}Cm	^{242}Pu	5.48	0	11.17	10.07	10.2	0.1424	11.05
^{238}Cf	^{234}Cm	8.13	0	1.02	−0.91	−0.76	0.0562	0.49
^{242}Cf	^{238}Cm	7.52	0	2.42	1.26	1.41	0.0636	2.61
^{246}Cf	^{242}Cm	6.86	0	5.11	3.84	3.99	0.0745	5.11
^{250}Cf	^{246}Cm	6.13	0	8.62	7.33	7.46	0.0927	8.49
^{254}Cf	^{250}Cm	5.93	0	9.22	8.31	8.45	0.0955	9.47
^{248}Fm	^{244}Cf	8	0	1.56	0.18	0.33	0.0477	1.65
^{254}Fm	^{250}Cf	7.31	0	4.07	2.67	2.81	0.0539	4.08
^{254}No	^{250}Fm	8.23	0	1.75	0.03	0.17	0.0387	1.58
^{258}No	^{254}Fm	8.15	0	2.08	0.24	0.37	0.0376	1.8
^{258}Rf	^{254}No	9.19	0	−0.98	−2.4	−2.26	0.0275	−0.7
^{260}Sg	^{256}Rf	9.9	0	−1.91	−3.77	−3.63	0.0218	−1.96
^{268}Hs	^{264}Sg	9.63	0	0.15	−2.44	−2.3	0.0195	−0.59
^{270}Ds	^{266}Hs	11.12	0	−3.69	−5.69	−5.55	0.014	−3.69
^{288}Fl	^{284}Cn	10.07	0	−0.12	−1.99	−1.87	0.0118	0.05
^{292}Lv	^{288}Fl	10.78	0	−1.62	−3.36	−3.23	0.0095	−1.21

Table 5. Same as Table 4, but for α decay of odd-A nuclei. Elements with superscript "m," "n," "p," or "x" indicate assignments to excited isomeric states (defined as higher states with half-lives greater than 100 ns). Elements with superscript "p" also indicate non-isomeric levels but are used in AME2016 [84, 85].

α transition		Q_α	l_{min}	$\lg T_{1/2}^{exp}$	$\lg T_{1/2}^{cal1}$	$\lg T_{1/2}^{cal2}$	P_α	$\lg T_{1/2}^{cal3}$
^{149}Tb	^{145}Eu	4.08	2	4.95	3.68	3.8	0.0841	4.88
^{151}Dy	^{147}Gd	4.18	0	4.28	3.19	3.25	0.0986	4.25
^{151}Ho	^{147}Tb^{m}	4.64	0	2.2	1.09	1.18	0.0838	2.25
^{153}Ho^{m}	^{149}Tb	4.12	0	5.47	4.14	4.27	0.1119	5.23
^{155}Er	^{151}Dy	4.12	0	6.15	4.74	4.86	0.119	5.79
^{153}Tm^{m}	^{149}Ho^{m}	5.24	0	0.43	−0.85	−0.72	0.0763	0.39
^{155}Yb	^{151}Er	5.34	0	0.3	−0.8	−0.65	0.0782	0.46
^{155}Lu	^{151}Tm	5.8	0	−1.12	−2.3	−2.14	0.0789	−1.04
^{155}Lu^{n}	^{151}Tm	7.58	8	−2.57	−4.48	−4.29	0.0181	−2.55
^{157}Hf	^{153}Yb	5.89	0	−0.91	−2.22	−2.08	0.0827	−0.99
^{159}Ta	^{155}Lu^{m}	5.66	0	0.48	−0.83	−0.6	0.1006	0.39
^{159}W	^{155}Hf	6.45	0	−2	−3.46	−3.23	0.0926	−2.2
^{163}W	^{159}Hf	5.52	0	1.27	0.24	0.4	0.0961	1.42
^{161}Re^{m}	^{157}Ta^{m}	6.43	0	−1.8	−2.97	−2.82	0.1018	−1.82
^{163}Re^{m}	^{159}Ta^{m}	6.07	0	−0.49	−1.63	−1.46	0.0975	−0.45
^{165}Re^{m}	^{161}Ta^{m}	5.66	0	1.12	0.02	0.22	0.0963	1.24
^{169}Re	^{165}Ta	5.01	3	5.18	3.79	3.99	0.0681	5.15
^{161}Os	^{157}W	7.07	0	−3.19	−4.74	−4.57	0.1068	−3.6
^{165}Os	^{161}W	6.34	0	−1.1	−2.28	−2.08	0.0951	−1.05
^{169}Os	^{165}W	5.71	0	1.4	0.21	0.42	0.0837	1.49
^{167}Ir	^{163}Re	6.51	0	−1.17	−2.51	−2.36	0.0971	−1.35
^{169}Ir	^{165}Re	6.14	0	−0.18	−1.13	−0.92	0.0916	0.11
^{171}Ir	^{167}Re^{m}	5.87	0	1.31	−0.05	0.06	0.0842	1.14
^{173}Ir^{m}	^{169}Re	5.94	2	1.26	−0.09	0.04	0.0562	1.29
^{177}Ir	^{173}Re	5.08	0	4.69	3.67	3.79	0.0664	4.97
^{171}Pt	^{167}Os	6.61	0	−1.3	−2.54	−2.43	0.0851	−1.36
^{175}Pt	^{171}Os	6.16	2	0.58	−0.57	−0.38	0.056	0.87
^{179}Pt	^{175}Os	5.41	2	3.94	2.72	2.81	0.0503	4.11
^{183}Pt	^{179}Os	4.82	0	6.61	5.57	5.69	0.0535	6.96
^{173}Au	^{169}Ir	6.84	0	−1.53	−2.96	−2.82	0.0863	−1.75
^{175}Au	^{171}Ir	6.59	0	−0.64	−2.08	−1.88	0.0773	−0.77
^{177}Au	^{173}Ir	6.3	0	0.56	−1	−0.89	0.0702	0.26
^{179}Au	^{175}Ir	5.98	1	1.51	0.35	0.44	0.0575	1.68
^{183}Au	^{179}Ir	5.47	0	3.89	2.59	2.7	0.053	3.98
^{171}Hg	^{167}Pt	7.67	2	−4.15	−4.9	−4.8	0.0898	−3.75
^{177}Hg	^{173}Pt	6.74	2	−0.82	−1.92	−1.82	0.0657	−0.64
^{181}Hg	^{177}Pt	6.28	2	1.12	−0.27	−0.09	0.0519	1.2
^{185}Hg	^{181}Pt	5.77	0	2.91	1.58	1.77	0.0511	3.06
^{177}Tl^{m}	^{173}Au^{m}	7.66	0	−3.44	−4.91	−4.78	0.0849	−3.71
^{179}Tl^{m}	^{175}Au^{m}	7.38	0	−2.85	−4.07	−3.93	0.0756	−2.81
^{151}Tb	^{147}Eu	3.5	2	8.82	7.76	7.79	0.1413	8.64
^{153}Dy	^{149}Gd	3.56	0	8.39	7.54	7.67	0.1652	8.45
^{151}Ho^{m}	^{147}Tb	4.74	0	1.79	0.6	0.7	0.0774	1.81
^{153}Er	^{149}Dy	4.8	0	1.84	0.78	0.91	0.0796	2
^{153}Tm	^{149}Ho	5.25	0	0.21	−0.87	−0.75	0.076	0.37
^{155}Tm	^{151}Ho	4.57	0	3.38	2.55	2.69	0.1032	3.67
^{157}Yb	^{153}Er	4.62	0	3.89	2.76	2.81	0.1057	3.78
^{155}Lu^{m}	^{151}Tm^{m}	5.73	0	−0.74	−2	−1.84	0.0821	−0.76
^{157}Lu^{m}	^{153}Tm	5.13	0	1.89	0.64	0.72	0.0967	1.73
^{157}Ta^{n}	^{153}Lu	7.95	8	−2.77	−4.75	−4.46	0.0246	−2.85
^{159}Ta^{m}	^{155}Lu	5.75	0	0.01	−1.19	−0.97	0.0964	0.05
^{161}W	^{157}Hf	5.92	0	−0.25	−1.46	−1.31	0.0963	−0.29
^{159}Re^{m}	^{155}Ta	6.97	0	−3.54	−4.8	−4.56	0.1005	−3.57
^{163}Re	^{159}Ta	6.01	0	0.08	−1.41	−1.24	0.0998	−0.24
^{165}Re	^{161}Ta	5.69	0	1.25	−0.13	0.08	0.0949	1.1
^{167}Re^{m}	^{163}Ta	5.41	0	2.77	1.17	1.29	0.0898	2.34
^{169}Re^{m}	^{165}Ta^{m}	5.16	3	3.88	3	3.19	0.0632	4.39
^{163}Os	^{159}W	6.69	0	−2.26	−3.5	−3.31	0.101	−2.32
^{167}Os	^{163}W	5.99	0	0.21	−0.93	−0.79	0.0903	0.25
^{165}Ir^{m}	^{161}Re^{m}	6.89	0	−2.57	−3.82	−3.6	0.1031	−2.62
^{167}Ir^{m}	^{163}Re^{m}	6.56	0	−1.55	−2.71	−2.56	0.0954	−1.54
^{169}Ir^{m}	^{165}Re^{m}	6.27	0	−0.45	−1.63	−1.42	0.0877	−0.37
^{171}Ir^{m}	^{167}Re	6.16	2	0.43	−0.94	−0.84	0.0625	0.37
^{175}Ir	^{171}Re	5.43	2	3.02	2.23	2.42	0.0567	3.67
^{167}Pt	^{163}Os	7.16	0	−3.1	−4.33	−4.17	0.104	−3.18
^{173}Pt	^{169}Os	6.36	0	−0.35	−1.64	−1.5	0.0767	−0.38
^{177}Pt	^{173}Os	5.64	0	2.27	1.36	1.48	0.0676	2.65
^{181}Pt	^{177}Os	5.15	0	4.85	3.74	3.93	0.0564	5.17
^{171}Au^{m}	^{167}Ir^{m}	7.16	0	−2.76	−4.04	−3.95	0.0947	−2.93
^{173}Au^{m}	^{169}Ir^{m}	6.9	0	−1.86	−3.17	−3.02	0.085	−1.95
^{175}Au^{m}	^{171}Ir^{m}	6.59	0	−0.75	−2.08	−1.88	0.0773	−0.77
^{177}Au^{m}	^{173}Ir^{m}	6.26	0	0.25	−0.85	−0.74	0.0709	0.41
^{181}Au	^{177}Ir	5.75	2	2.7	1.56	1.75	0.0475	3.07
^{185}Au	^{181}Ir	5.18	0	4.98	4.05	4.23	0.0488	5.54
^{173}Hg	^{169}Pt	7.38	2	−3.1	−4.04	−3.88	0.0804	−2.79
^{179}Hg	^{175}Pt	6.36	0	0.14	−0.86	−0.76	0.0737	0.37
^{183}Hg	^{179}Pt	6.04	0	1.9	0.42	0.53	0.0566	1.78
^{177}Tl	^{173}Au	7.07	0	−1.61	−2.97	−2.88	0.0951	−1.86
^{179}Tl	^{175}Au	6.71	0	−0.36	−1.75	−1.64	0.0863	−0.57
^{181}Tl^{m}	^{177}Au^{m}	6.97	2	−0.46	−2.42	−2.23	0.0567	−0.99

Continued on next page

Table 5-continued from previous page

α transition		Q_α	l_{min}	$\lg T_{1/2}^{exp}$	$\lg T_{1/2}^{cal1}$	$\lg T_{1/2}^{cal2}$	P_α	$\lg T_{1/2}^{cal3}$
^{183}Tl	^{179}Au	5.98	0	2.54	1.16	1.28	0.072	2.42
^{187}Tl^{m}	^{183}Au	5.66	2	4	2.87	3.05	0.0453	4.39
^{183}Pb^{m}	^{179}Hg	7.02	3	−0.38	−1.93	−1.83	0.0555	−0.58
^{187}Pb	^{183}Hg	6.39	2	2.2	0.06	0.24	0.0482	1.56
^{189}Pb	^{185}Hg	5.92	2	3.99	2.1	2.21	0.0447	3.56
^{187}Bi	^{183}Tl	7.78	5	−1.43	−3.24	−3.07	0.0385	−1.65
^{189}Bi	^{185}Tl	7.27	5	−0.18	−1.64	−1.54	0.0351	−0.09
^{191}Bi^{m}	^{187}Tl	7.02	0	−0.78	−2.26	−2.08	0.048	−0.76
^{193}Bi^{m}	^{189}Tl	6.61	0	0.56	−0.8	−0.61	0.0433	0.75
^{195}Bi^{m}	^{191}Tl	6.23	0	2.42	0.73	0.92	0.0389	2.33
^{211}Bi	^{207}Tl	6.75	5	2.11	−0.21	−0.05	0.0287	1.49
^{187}Po	^{183}Pb	7.98	2	−2.85	−4.61	−4.42	0.061	−3.21
^{195}Po	^{191}Pb	6.75	0	0.69	−0.89	−0.71	0.0451	0.64
^{197}Po	^{193}Pb	6.41	0	2.08	0.43	0.61	0.04	2.01
^{199}Po	^{195}Pb	6.08	0	3.64	1.84	2.02	0.0355	3.47
^{201}Po	^{197}Pb	5.8	0	4.92	3.05	3.23	0.0313	4.74
^{203}Po	^{199}Pb	5.5	2	6.29	4.86	5.02	0.0227	6.66
^{205}Po	^{201}Pb	5.33	0	7.18	5.46	5.63	0.0241	7.25
^{209}Po	^{205}Pb^{m}	4.98	0	9.59	7.46	7.62	0.0183	9.36
^{213}Po	^{209}Pb	8.54	0	−5.43	−6.94	−6.75	0.0666	−5.57
^{219}Po	^{215}Pb	5.92	0	3.34	2.19	2.35	0.0834	3.43
^{191}At^{m}	^{187}Bi	7.88	2	−2.66	−4	−3.81	0.0566	−2.56
^{193}At^{m}	^{189}Bi	7.58	2	−1.68	−3.11	−2.92	0.0497	−1.62
^{195}At	^{191}Bi^{m}	7.1	0	−0.54	−1.79	−1.6	0.054	−0.33
^{197}At^{m}	^{193}Bi^{m}	6.84	0	0.3	−0.87	−0.69	0.0472	0.63
^{199}At^{m}	^{195}Bi	7.02	5	1.44	−0.12	0.04	0.0255	1.64
^{203}At	^{199}Bi	6.21	0	3.15	1.6	1.76	0.0312	3.27
^{207}At	^{203}Bi	5.87	0	4.81	3.12	3.29	0.0235	4.92
^{211}At	^{207}Bi	5.98	0	4.79	2.49	2.66	0.0171	4.42
^{215}At	^{211}Bi	8.18	0	−4	−5.6	−5.45	0.0663	−4.27
^{219}At	^{215}Bi	6.34	0	1.78	0.74	0.91	0.0781	2.02
^{195}Rn	^{191}Po	7.69	0	−2.15	−3.39	−3.2	0.0642	−2
^{197}Rn	^{193}Po	7.41	0	−1.27	−2.49	−2.31	0.056	−1.06
^{203}Rn	^{199}Po	6.63	0	1.82	0.29	0.45	0.0369	1.88
^{205}Rn	^{201}Po	6.39	2	2.84	1.57	1.74	0.0263	3.32
^{209}Rn	^{205}Po	6.16	0	4	2.25	2.41	0.0239	4.03
^{213}Rn	^{209}Po	8.25	5	−1.71	−4.03	−3.86	0.0224	−2.21
^{217}Rn	^{213}Po	7.89	0	−3.27	−4.38	−4.21	0.0656	−3.03
^{221}Rn	^{217}Po	6.16	2	3.84	2.27	2.44	0.0455	3.78
^{197}Fr	^{193}At^{m}	7.88	0	−2.63	−3.64	−3.45	0.0677	−2.29
^{199}Fr^{m}	^{195}At^{m}	7.83	0	−2.19	−3.5	−3.32	0.0581	−2.09
^{201}Fr^{m}	^{197}At^{m}	7.6	0	−1.77	−2.81	−2.63	0.0504	−1.33
^{183}Tl^{m}	^{179}Au	6.61	3	0.54	−0.83	−0.72	0.0474	0.6
^{179}Pb	^{175}Hg	7.6	2	−2.41	−4.06	−3.93	0.0764	−2.81
^{185}Pb^{m}	^{181}Hg^{m}	6.56	0	0.91	−0.82	−0.63	0.0674	0.54
^{187}Pb^{m}	^{183}Hg^{m}	6.21	0	2.18	0.53	0.71	0.0609	1.93
^{191}Pb^{m}	^{187}Hg^{m}	5.4	0	5.82	4.29	4.47	0.0512	5.76
^{187}Bi^{m}	^{183}Tl	7.89	0	−3.43	−5.02	−4.82	0.0591	−3.59
^{191}Bi	^{187}Tl^{m}	6.45	0	1.36	−0.07	0.12	0.0522	1.4
^{193}Bi	^{189}Tl^{m}	6.02	0	3.26	1.68	1.86	0.0474	3.19
^{195}Bi	^{191}Tl^{m}	5.54	0	5.76	4.01	4.19	0.0436	5.55
^{209}Bi	^{205}Tl	3.14	5	26.8	24.29	24.43	0.0145	26.27
^{213}Bi	^{209}Tl	5.99	5	5.12	2.96	3.12	0.031	4.63
^{189}Po	^{185}Pb	7.69	2	−2.42	−3.78	−3.68	0.0536	−2.41
^{195}Po^{m}	^{191}Pb^{m}	6.84	0	0.33	−1.26	−1.07	0.0446	0.28
^{197}Po^{m}	^{193}Pb^{m}	6.51	0	1.48	0.02	0.2	0.0395	1.6
^{199}Po^{m}	^{195}Pb^{m}	6.18	0	3.02	1.36	1.53	0.035	2.99
^{201}Po^{m}	^{197}Pb^{m}	5.9	0	4.34	2.55	2.73	0.0309	4.24
^{203}Po^{m}	^{199}Pb	6.14	5	5.05	2.92	3.07	0.0165	4.85
^{207}Po	^{203}Pb	5.22	0	7.99	6.06	6.23	0.0208	7.91
^{211}Po^{m}	^{207}Pb	9.06	13	1.4	−0.66	−0.53	0.0037	1.9
^{215}Po	^{211}Pb	7.53	0	−2.75	−3.99	−3.84	0.0714	−2.69
^{191}At	^{187}Bi^{m}	7.71	0	−2.68	−3.77	−3.58	0.0701	−2.42
^{193}At	^{189}Bi^{m}	7.39	0	−1.54	−2.76	−2.58	0.0616	−1.37
^{193}At^{n}	^{189}Bi	7.62	3	−0.93	−2.93	−2.75	0.0456	−1.41
^{197}At	^{193}Bi	7.11	0	−0.39	−1.84	−1.66	0.0461	−0.32
^{199}At	^{195}Bi	6.78	0	0.89	−0.64	−0.46	0.0405	0.93
^{201}At	^{197}Bi	6.47	0	2.07	0.51	0.69	0.0356	2.14
^{205}At	^{201}Bi	6.02	0	4.3	2.45	2.62	0.0271	4.18
^{209}At	^{205}Bi	5.76	0	5.67	3.66	3.83	0.0203	5.52
^{213}At	^{209}Bi	9.25	0	−6.9	−8.4	−8.2	0.0623	−7
^{217}At	^{213}Bi	7.2	0	−1.49	−2.52	−2.35	0.0716	−1.2
^{193}Rn	^{189}Po	8.04	2	−2.94	−4.15	−3.96	0.0601	−2.74
^{195}Rn^{m}	^{191}Po^{m}	7.71	0	−2.22	−3.45	−3.26	0.0641	−2.07
^{197}Rn^{m}	^{193}Po^{m}	7.51	0	−1.59	−2.82	−2.64	0.0556	−1.39
^{203}Rn^{m}	^{199}Po^{m}	6.68	0	1.55	0.08	0.24	0.0368	1.67
^{207}Rn	^{203}Po	6.25	0	3.42	1.84	2.02	0.0277	3.57
^{211}Rn	^{207}Po	5.97	2	5.28	3.34	3.5	0.017	5.27
^{215}Rn	^{211}Po	8.84	0	−5.64	−7.06	−6.9	0.0621	−5.69
^{219}Rn	^{215}Po	6.95	2	0.6	−0.95	−0.78	0.0419	0.59
^{223}Rn	^{219}Po	5.28	2	8.56	6.73	6.88	0.0526	8.16
^{199}Fr	^{195}At	7.82	0	−2.18	−3.45	−3.27	0.0582	−2.03
^{201}Fr	^{197}At	7.52	0	−1.2	−2.54	−2.35	0.0506	−1.06
^{203}Fr	^{199}At	7.27	0	−0.26	−1.73	−1.56	0.0439	−0.2

Table 5-continued from previous page

α transition		Q_α	l_{min}	$\lg T_{1/2}^{exp}$	$\lg T_{1/2}^{cal1}$	$\lg T_{1/2}^{cal2}$	P_α	$\lg T_{1/2}^{cal3}$
^{203}Fr^{m}	^{199}At^{m}	7.39	0	−0.68	−2.14	−1.97	0.0436	−0.61
^{207}Fr	^{203}At	6.89	0	1.19	−0.37	−0.19	0.0328	1.29
^{211}Fr	^{207}At	6.66	0	2.33	0.45	0.61	0.0244	2.23
^{215}Fr	^{211}At	9.54	0	−7.07	−8.42	−8.26	0.0582	−7.03
^{221}Fr	^{217}At	6.46	2	2.46	1.43	1.59	0.0439	2.95
^{201}Ra	^{197}Rn	8	0	−1.7	−3.7	−3.51	0.0616	−2.3
^{203}Ra	^{199}Rn	7.74	0	−1.44	−2.89	−2.72	0.0533	−1.45
^{207}Ra	^{203}Rn	7.27	2	0.21	−1.06	−0.88	0.0327	0.6
^{213}Ra	^{209}Rn	6.86	2	2.31	0.35	0.52	0.0209	2.2
^{217}Ra	^{213}Rn	9.16	0	−5.79	−7.22	−7.04	0.0575	−5.8
^{221}Ra	^{217}Rn	6.88	2	1.45	0.14	0.31	0.0414	1.69
^{205}Ac	^{201}Fr^{n}	7.9	3	−1.1	−2.48	−2.31	0.0427	−0.94
^{211}Ac	^{207}Fr	7.62	0	−0.67	−2.25	−2.08	0.0361	−0.64
^{217}Ac	^{213}Fr	9.83	0	−7.16	−8.45	−8.27	0.0542	−7
^{219}Ac	^{215}Fr	8.83	0	−4.93	−6.04	−5.86	0.0567	−4.61
^{223}Ac	^{219}Fr	6.78	2	2.1	0.93	1.08	0.04	2.48
^{227}Ac	^{223}Fr	5.04	0	10.7	9.38	9.54	0.0897	10.59
^{215}Th	^{211}Ra	7.67	2	0.08	−1.79	−1.65	0.027	−0.08
^{219}Th	^{215}Ra	9.51	0	−5.99	−7.44	−7.26	0.0531	−5.98
^{223}Th	^{219}Ra	7.57	2	−0.22	−1.6	−1.44	0.0354	0.01
^{227}Th	^{223}Ra	6.15	2	6.21	4.08	4.24	0.0402	5.64
^{231}Th	^{227}Ra	4.21	2	17.36	16.34	16.48	0.063	17.68
^{215}Pa	^{211}Ac	8.24	0	−1.85	−3.52	−3.37	0.0409	−1.98
^{221}Pa	^{217}Ac	9.25	0	−5.23	−6.48	−6.29	0.0517	−5.01
^{227}Pa	^{223}Ac	6.58	0	3.43	2.29	2.45	0.0634	3.65
^{219}U	^{215}Th	9.94	5	−4.26	−6.51	−6.34	0.0161	−4.55
^{225}U	^{221}Th	8.02	2	−1.21	−2.34	−2.18	0.0317	−0.68
^{229}U	^{225}Th	6.48	0	4.24	3.18	3.33	0.0614	4.54
^{233}U	^{229}Th	4.91	0	12.7	11.87	12.02	0.0808	13.11
^{229}Np	^{225}Pa	7.02	1	2.55	1.41	1.56	0.0414	2.95
^{235}Np	^{231}Pa	5.19	1	12.12	10.52	10.64	0.0515	11.93
^{239}Np	^{235}Pa	4.6	1	16.61	14.68	14.82	0.0542	16.08
^{233}Pu	^{229}U	6.41	2	6	4.61	4.76	0.0329	6.24
^{239}Pu	^{235}U^{xm}	5.24	0	11.88	10.6	10.74	0.0604	11.96
^{229}Am	^{225}Np	8.14	2	0.3	−1.67	−1.51	0.0282	0.04
^{235}Am	^{231}Np	6.59	1	5.18	4.01	4.14	0.0374	5.57
^{239}Am	^{235}Np	5.92	1	8.63	7.24	7.38	0.0375	8.81
^{243}Am	^{239}Np	5.44	1	11.37	9.96	10.1	0.0368	11.53
^{237}Cm	^{233}Pu	6.78	0	4.82	3.5	3.64	0.0459	4.98
^{243}Cm	^{239}Pu	6.17	2	8.96	6.57	6.71	0.0246	8.32
^{247}Bk	^{243}Am	5.89	2	10.64	8.43	8.56	0.0232	10.2
^{243}Cf	^{239}Cm	7.42	3	3.66	2.16	2.29	0.0156	4.1
^{205}Fr	^{201}At	7.05	0	0.58	−0.95	−0.78	0.038	0.64
^{209}Fr	^{205}At	6.78	0	1.75	0.06	0.23	0.0283	1.78
^{213}Fr	^{209}At	6.91	0	1.54	−0.53	−0.36	0.0209	1.32
^{219}Fr	^{215}At	7.45	0	−1.7	−2.62	−2.45	0.0667	−1.27
^{223}Fr	^{219}At	5.56	4	7.34	6.36	6.51	0.0324	8
^{201}Ra^{m}	^{197}Rn^{m}	8.07	0	−2.22	−3.89	−3.71	0.0615	−2.5
^{203}Ra^{m}	^{199}Rn^{m}	7.76	0	−1.6	−2.98	−2.81	0.0533	−1.54
^{209}Ra	^{205}Rn	7.14	0	0.67	−0.91	−0.74	0.0343	0.72
^{215}Ra	^{211}Rn	8.86	5	−2.78	−5.09	−4.96	0.0199	−3.25
^{219}Ra	^{215}Rn	8.14	2	−2	−4.17	−3.99	0.0361	−2.55
^{223}Ra	^{219}Rn	5.98	2	5.99	4.04	4.2	0.0465	5.53
^{207}Ac	^{203}Fr	7.85	0	−1.51	−2.92	−2.74	0.0486	−1.42
^{215}Ac	^{211}Fr	7.75	0	−0.77	−2.73	−2.59	0.0269	−1.02
^{217}Ac^{m}	^{213}Fr	11.84	11	−4.77	−7.07	−6.93	0.0037	−4.5
^{221}Ac	^{217}Fr	7.78	0	−1.28	−2.95	−2.78	0.0612	−1.56
^{225}Ac	^{221}Fr	5.94	2	5.93	4.72	4.87	0.0446	6.23
^{209}Th^{m}	^{205}Ra^{m}	8.28	0	−2.51	−3.91	−3.73	0.0517	−2.45
^{217}Th	^{213}Ra	9.44	5	−3.61	−5.9	−5.74	0.0178	−3.99
^{221}Th	^{217}Ra	8.63	2	−2.75	−4.87	−4.7	0.0324	−3.21
^{225}Th	^{221}Ra	6.92	2	2.77	0.78	0.94	0.0368	2.38
^{229}Th	^{225}Ra	5.17	2	11.4	9.4	9.54	0.0484	10.86
^{213}Pa	^{209}Ac	8.4	0	−2.15	−3.97	−3.79	0.0476	−2.47
^{217}Pa	^{213}Ac	8.49	0	−2.46	−4.31	−4.14	0.0357	−2.7
^{223}Pa	^{219}Ac	8.33	0	−2.29	−3.93	−3.77	0.0543	−2.5
^{229}Pa	^{225}Ac	5.84	1	7.43	5.91	6.06	0.0515	7.34
^{221}U	^{217}Th	9.89	0	−6.18	−7.68	−7.5	0.0487	−6.19
^{227}U	^{223}Th	7.23	2	1.82	0.34	0.5	0.0335	1.98
^{231}U	^{227}Th	5.58	2	9.95	7.99	8.13	0.0419	9.51
^{227}Np	^{223}Pa	7.82	2	−0.29	−1.34	−1.18	0.0309	0.33
^{231}Np	^{227}Pa	6.36	1	5.14	4.22	4.37	0.044	5.72
^{237}Np	^{233}Pa	4.96	1	13.83	12.07	12.21	0.0515	13.49
^{231}Pu	^{227}U	6.84	0	3.58	2.46	2.61	0.055	3.87
^{235}Pu	^{231}U	5.95	0	7.72	6.55	6.67	0.0577	7.91
^{241}Pu	^{237}U	5.14	2	13.26	11.54	11.68	0.034	13.15
^{233}Am	^{229}Np	7.06	1	3.62	2.07	2.22	0.0366	3.66
^{237}Am	^{233}Np	6.2	1	7.24	5.84	5.99	0.0378	7.41
^{241}Am	^{237}Np	5.64	1	10.14	8.8	8.95	0.0375	10.37
^{233}Cm	^{229}Pu	7.47	0	2.13	0.78	0.94	0.0468	2.27
^{241}Cm	^{237}Pu	6.19	3	8.45	6.78	6.93	0.0213	8.6
^{245}Cm	^{241}Pu	5.62	2	11.42	9.46	9.59	0.0264	11.17
^{241}Cf	^{237}Cm^{p}	7.46	0	2.75	1.51	1.66	0.0354	3.11
^{245}Cf	^{241}Cm	7.26	0	3.87	2.18	2.32	0.0314	3.83

Table 5-continued from previous page

α transition		Q_α	l_{min}	$\lg T_{1/2}^{exp}$	$\lg T_{1/2}^{cal1}$	$\lg T_{1/2}^{cal2}$	P_α	$\lg T_{1/2}^{cal3}$	α transition		Q_α	l_{min}	$\lg T_{1/2}^{exp}$	$\lg T_{1/2}^{cal1}$	$\lg T_{1/2}^{cal2}$	P_α	$\lg T_{1/2}^{cal3}$
^{247}Cf	^{243}Cm	6.5	2	7.5	5.78	5.92	0.0203	7.61	^{251}Cf	^{247}Cm	6.18	5	10.45	8.38	8.51	0.0098	10.52
^{245}Es	^{241}Bk^{p}	7.87	0	2.22	0.28	0.42	0.0285	1.97	^{247}Es	^{243}Bk^{p}	7.44	1	3.59	1.93	2.08	0.021	3.75
^{249}Es	^{245}Bk^{p}	6.9	1	6.03	4.2	4.34	0.0218	6	^{253}Es	^{249}Bk	6.74	0	6.25	4.77	4.91	0.0262	6.49
^{255}Es	^{251}Bk^{m}	6.4	0	7.63	6.3	6.44	0.0263	8.02	^{243}Fm	^{239}Cf	8.7	1	−0.6	−1.98	−1.83	0.0201	−0.14
^{247}Fm	^{243}Cf	8.26	4	1.69	0.13	0.27	0.0095	2.29	^{247}Fm^{m}	^{243}Cf	8.31	0	0.76	−0.88	−0.73	0.0248	0.87
^{253}Fm	^{249}Cf^{m}	7.05	2	6.33	4.07	4.21	0.0147	6.04	^{257}Fm	^{253}Cf	6.86	2	6.94	4.81	4.93	0.0131	6.82
^{247}Md	^{243}Es	8.77	1	0.08	−1.91	−1.76	0.0172	0.004	^{247}Md^{m}	^{243}Es	9.03	3	−0.5	−2.29	−2.14	0.0106	−0.17
^{251}Md	^{247}Es	7.96	1	3.4	0.73	0.86	0.0169	2.64	^{251}No	^{247}Fm	8.76	0	−0.02	−1.65	−1.51	0.0203	0.18
^{251}No^{m}	^{247}Fm^{m}	8.82	0	0.01	−1.84	−1.7	0.0201	−0.003	^{253}No	^{249}Fm	8.42	1	2.23	−0.48	−0.34	0.0146	1.5
^{255}No	^{251}Fm^{m}	8.23	2	2.84	0.26	0.4	0.0112	2.35	^{259}No	^{255}Fm	7.85	2	3.66	1.56	1.69	0.0102	3.68
^{253}Lr	^{249}Md	8.93	0	−0.15	−1.84	−1.7	0.0185	0.03	^{253}Lr^{m}	^{249}Md^{m}	8.86	0	0.17	−1.62	−1.48	0.0187	0.25
^{255}Lr	^{251}Md^{p}	8.5	0	1.49	−0.54	−0.4	0.0183	1.34	^{257}Lr	^{253}Md	9.08	4	0.78	−1.58	−1.45	0.0059	0.78
^{259}Lr	^{255}Md^{p}	8.58	0	0.9	−0.83	−0.7	0.0155	1.11	^{255}Rf	^{251}No	9.06	1	0.54	−1.86	−1.71	0.0125	0.19
^{257}Rf^{m}	^{253}No	9.16	2	0.69	−2.03	−1.9	0.0091	0.14	^{259}Rf	^{255}No^{p}	9.03	0	0.46	−1.9	−1.76	0.0146	0.07
^{261}Rf	^{257}No	8.65	0	0.9	−0.72	−0.59	0.0144	1.26	^{263}Rf	^{259}No	8.26	4	3.34	1.36	1.5	0.0054	3.77
^{259}Db	^{255}Lr^{m}	9.58	1	−0.29	−3.11	−2.97	0.01	−0.97	^{259}Sg	^{255}Rf	9.77	2	−0.38	−3.14	−3	0.0079	−0.9
^{259}Sg^{m}	^{255}Rf^{m}	9.71	2	−0.63	−2.97	−2.84	0.008	−0.74	^{261}Sg	^{257}Rf	9.71	2	−0.73	−3.02	−2.88	0.0074	−0.75
^{263}Sg	^{259}Rf	9.41	0	0.03	−2.41	−2.27	0.0121	−0.35	^{261}Bh	^{257}Db	10.5	3	−1.87	−4.53	−4.39	0.0054	−2.12
^{265}Hs	^{261}Sg	10.47	0	−2.71	−4.7	−4.56	0.0099	−2.56	^{269}Hs	^{265}Sg	9.35	0	1.2	−1.62	−1.48	0.0099	0.52
^{267}Ds	^{263}Hs	11.78	0	−5	−7.1	−6.96	0.0079	−4.85	^{269}Ds	^{265}Hs^{m}	11.28	0	−3.64	−6.04	−5.9	0.0078	−3.79
^{271}Ds	^{267}Hs	10.88	5	−1.05	−4.01	−3.88	0.0023	−1.24	^{271}Ds^{m}	^{267}Hs	10.95	2	−2.77	−5.08	−4.94	0.0044	−2.58
^{273}Ds	^{269}Hs	11.38	3	−3.62	−5.92	−5.79	0.0031	−3.28	^{277}Ds	^{273}Hs	10.83	4	−2.22	−4.39	−4.26	0.0023	−1.62
^{277}Cn	^{273}Ds^{m}	11.42	0	−3.07	−5.9	−5.76	0.0057	−3.52	^{281}Cn	^{277}Ds	10.46	4	−0.74	−2.87	−2.75	0.0021	−0.07
^{289}Fl	^{285}Cn	9.97	0	0.38	−1.72	−1.6	0.0044	0.76									

Table 6. Same as Tables 4 and 5, but for α decay of doubly odd nuclei.

α transition		Q_α	l_{min}	$\lg T_{1/2}^{exp}$	$\lg T_{1/2}^{cal1}$	$\lg T_{1/2}^{cal2}$	P_α	$\lg T_{1/2}^{cal3}$	α transition		Q_α	l_{min}	$\lg T_{1/2}^{exp}$	$\lg T_{1/2}^{cal1}$	$\lg T_{1/2}^{cal2}$	P_α	$\lg T_{1/2}^{cal3}$
^{148}Eu	^{144}Pm	2.69	0	14.98	13.77	13.95	0.0795	15.04	^{152}Ho	^{148}Tb	4.51	0	3.12	1.83	1.95	0.0634	3.14
^{152}Ho^{m}	^{148}Tb^{m}	4.58	0	2.66	1.44	1.56	0.0635	2.76	^{154}Ho	^{150}Tb	4.04	0	6.56	4.65	4.88	0.0582	6.11
^{154}Tm	^{150}Ho	5.09	0	1.17	−0.16	0.08	0.059	1.3	^{154}Tm^{m}	^{150}Ho^{m}	5.18	0	0.75	−0.54	−0.31	0.0592	0.92
^{156}Tm	^{152}Ho	4.35	0	5.12	3.88	4.03	0.0533	5.3	^{156}Lu^{m}	^{152}Tm^{m}	5.72	0	−0.68	−1.96	−1.78	0.0558	−0.53
^{158}Ta	^{154}Lu	6.13	0	−1.29	−2.71	−2.62	0.0526	−1.34	^{158}Ta^{m}	^{154}Lu^{m}	6.21	0	−1.42	−3.01	−2.91	0.0528	−1.63
^{160}Re	^{156}Ta	6.7	2	−2.26	−3.6	−3.46	0.0303	−1.94	^{162}Re	^{158}Ta	6.25	0	−0.95	−2.32	−2.15	0.0456	−0.81
^{162}Re^{m}	^{158}Ta^{m}	6.28	0	−1.07	−2.43	−2.26	0.0457	−0.92	^{164}Re^{m}	^{160}Ta^{m}	5.77	0	1.46	−0.43	−0.22	0.0411	1.16
^{164}Ir^{m}	^{160}Re^{m}	7.06	0	−2.78	−4.36	−4.15	0.0445	−2.8	^{166}Ir	^{162}Re	6.73	0	−1.95	−3.29	−3.15	0.0405	−1.76
^{166}Ir^{m}	^{162}Re^{m}	6.73	0	−1.81	−3.29	−3.15	0.0405	−1.76	^{168}Ir	^{164}Re	6.38	0	−0.64	−2.03	−1.9	0.0368	−0.46
^{168}Ir^{m}	^{164}Re^{m}	6.48	0	−0.68	−2.41	−2.27	0.0371	−0.84	^{170}Ir	^{166}Re^{p}	5.96	0	1.24	−0.37	−0.17	0.0332	1.31
^{170}Ir^{m}	^{166}Re	6.27	2	0.35	−1.32	−1.12	0.0205	0.57	^{172}Ir	^{168}Re	5.99	3	2.34	0.06	0.16	0.0151	1.98
^{172}Ir^{m}	^{168}Re	6.13	0	1.36	−1.16	−1.04	0.0314	0.46	^{174}Ir	^{170}Re	5.63	2	3.17	1.31	1.5	0.0168	3.27
^{174}Ir^{m}	^{170}Re	5.82	2	2.29	0.44	0.63	0.0172	2.4	^{170}Au	^{166}Ir	7.18	0	−2.58	−4.03	−3.82	0.0362	−2.38

Continued on next page

Table 6-continued from previous page

α transition		Q_α	$l_{\min}$	$\lg T_{1/2}^{\rm exp}$	$\lg T_{1/2}^{\rm cal1}$	$\lg T_{1/2}^{\rm cal2}$	P_α	$\lg T_{1/2}^{\rm cal3}$
^{170}Au^{m}	^{166}Ir^{m}	7.29	0	−2.84	−4.38	−4.17	0.0365	−2.74
^{186}Au	^{182}Ir	4.91	1	7.89	5.59	5.77	0.0122	7.69
^{186}Tl^{m}	^{182}Au	6.02	6	5.66	3.01	3.18	0.0048	5.5
^{186}Bi^{m}	^{182}Tl^{m}	7.88	3	−2.01	−4.38	−4.19	0.0107	−2.22
^{190}Bi^{m}	^{186}Tl^{m}	6.97	3	0.94	−1.45	−1.35	0.0086	0.72
^{192}Bi^{m}	^{188}Tl^{m}	6.49	3	2.58	0.36	0.54	0.0076	2.66
^{194}Bi^{n}	^{190}Tl^{m}	6.02	3	4.74	2.31	2.48	0.0067	4.66
^{196}Bi^{n}	^{192}Tl^{n}	5.32	2	7.8	5.45	5.56	0.0069	7.72
^{214}Bi	^{210}Tl	5.62	5	6.75	4.73	4.89	0.0091	6.93
^{192}At^{m}	^{188}Bi^{m}	7.63	3	−1.06	−2.94	−2.76	0.0085	−0.69
^{194}At^{m}	^{190}Bi^{m}	7.31	0	−0.49	−2.49	−2.3	0.0157	−0.5
^{200}At^{n}	^{196}Bi^{m}	6.77	3	1.88	−0.05	0.12	0.0059	2.35
^{202}At^{m}	^{198}Bi^{m}	6.26	0	3.32	1.4	1.51	0.0106	3.48
^{204}At	^{200}Bi	6.07	0	4.16	2.22	2.38	0.0097	4.4
^{208}At	^{204}Bi	5.75	0	6.02	3.7	3.82	0.0081	5.91
^{212}At	^{208}Bi	7.82	5	−0.5	−3.1	−2.93	0.0061	−0.72
^{220}At	^{216}Bi^{m}	6.05	0	3.43	2.02	2.18	0.0542	3.45
^{212}Fr	^{208}At	6.53	2	3.44	1.27	1.44	0.0047	3.77
^{218}Fr	^{214}At	8.01	0	−3	−4.43	−4.26	0.0513	−2.97
^{220}Fr	^{216}At	6.8	1	1.44	−0.16	0.01	0.0289	1.55
^{216}Ac^{m}	^{212}Fr	9.28	5	−3.36	−5.84	−5.68	0.006	−3.46
^{222}Ac	^{218}Fr	7.14	0	0.7	−0.72	−0.56	0.0548	0.7
^{220}Pa	^{216}Ac	9.65	0	−6.11	−7.45	−7.27	0.0698	−6.11
^{228}Pa	^{224}Ac	6.27	3	6.63	4.25	4.36	0.0078	6.47
^{242}Am^{m}	^{238}Np	5.64	3	11.99	9.26	9.4	0.0018	12.15
^{248}Es	^{244}Bk	7.16	2	5.76	3.24	3.38	0.0024	6
^{254}Es^{m}	^{250}Bk	6.7	1	7.64	4.96	5.1	0.0016	7.9
^{258}Md	^{254}Es	7.27	1	6.65	3.29	3.42	0.0014	6.27
^{176}Au	^{172}Ir	6.44	0	0.14	−1.52	−1.32	0.0277	0.24
^{180}Tl	^{176}Au^{m}	6.57	3	1.23	−0.62	−0.43	0.0117	1.5
^{186}Bi	^{182}Tl	7.76	1	−1.83	−4.51	−4.32	0.0162	−2.53
^{190}Bi	^{186}Tl	6.86	1	0.91	−1.56	−1.46	0.013	0.43
^{192}Bi	^{188}Tl	6.38	1	2.44	0.29	0.47	0.0115	2.41
^{194}Bi	^{190}Tl	5.92	1	4.31	2.25	2.43	0.0101	4.42
^{196}Bi	^{192}Tl^{p}	5.26	0	7.42	5.46	5.57	0.0114	7.51
^{212}Bi	^{208}Tl	6.21	5	4	1.99	2.15	0.0085	4.22
^{192}At	^{188}Bi	7.7	0	−1.94	−3.72	−3.54	0.0175	−1.78
^{194}At	^{190}Bi^{n}	7.33	0	−0.54	−2.59	−2.4	0.0158	−0.6
^{200}At	^{196}Bi	6.6	0	1.92	0.06	0.24	0.0119	2.17
^{202}At	^{198}Bi	6.35	0	3.16	0.99	1.1	0.0108	3.07
^{202}At^{n}	^{198}Bi^{n}	6.4	0	2.68	0.79	0.9	0.0109	2.86
^{206}At	^{202}Bi	5.89	0	5.31	3.06	3.23	0.0088	5.29
^{210}At	^{206}Bi	5.63	2	7.22	4.52	4.68	0.0045	7.03
^{218}At	^{214}Bi	6.87	0	0.18	−1.38	−1.21	0.0501	0.09
^{200}Fr^{m}	^{196}At^{m}	7.71	0	−0.72	−3.11	−2.92	0.0133	−1.05
^{214}Fr	^{210}At	8.59	5	−2.29	−4.66	−4.49	0.0058	−2.25
^{218}Fr^{m}	^{214}At^{n}	7.87	2	−1.66	−3.7	−3.53	0.017	−1.76
^{216}Ac	^{212}Fr	9.24	5	−3.36	−5.74	−5.57	0.0061	−3.36
^{218}Ac	^{214}Fr	9.37	0	−6	−7.43	−7.25	0.0595	−6.02
^{226}Ac	^{222}Fr	5.51	2	9.23	6.98	7.13	0.0156	8.94
^{224}Pa	^{220}Ac	7.69	2	−0.07	−1.64	−1.48	0.017	0.29
^{230}Pa	^{226}Ac	5.44	2	10.67	8.27	8.41	0.011	10.37
^{246}Es	^{242}Bk^{p}	7.5	0	3.66	1.65	1.79	0.0101	3.79
^{252}Es	^{248}Bk	6.79	2	7.72	4.83	4.96	0.0013	7.85
^{256}Md^{m}	^{252}Es	7.91	3	4.7	1.27	1.41	0.0008	4.5

numbers are close to the $N = 126$ closed shell and the superheavy nuclei region, the deviations caused by $\lg T_{1/2}^{\rm cal1}$ and $\lg T_{1/2}^{\rm cal2}$ have maximum values, indicating that there are important physics, such as the shell effect, which need to be considered. This also indicates that changing the proximity energy does not affect the revealing of the microscopic shell effect, which is important for predicting the island of stability for superheavy nuclei. After considering the α-particle preformation factors obtained using Eq. (3), the deviations caused by $\lg T_{1/2}^{\rm cal3}$ are approximately zero, indicating that the accuracy of the calculations has been significantly improved. For all 535 nuclei, the RMS deviation between $\lg T_{1/2}^{\rm cal3}$ and $\lg T_{1/2}^{\rm exp}$ is $\sigma = 0.258$, indicating that the calculated α decay half-lives using the GLDM with proximity energy Prox. 77-Set 13 and the α-particle preformation factor estimated by Eq. (3) can reproduce the experimental data within a factor of $10^{0.258} = 1.81$. In addition, as can be seen from Figs. 2-4, $\lg T_{1/2}^{\rm cal2}$ is approximately 0.2 larger than $\lg T_{1/2}^{\rm cal1}$ on the whole, indicating that the introduction of proximity energy Prox. 77-Set 13 systematically improves the calculated accuracy of the GLDM to describe the α decay half-lives. Fig. 5 shows the deviations between the calculations by the GLDM with proximity energy Prox. 77-Set 13 and that with the original one for even-even heavy and superheavy nuclei. In this figure, it is seen that the deviations are approximately 0.2 and 0.14 in the heavy and superheavy nuclei regions, respectively. This indicates that compared with the heavy nuclei, in the superheavy nuclei region, the α decay half-life is less sensitive to the proximity energy, which helps us to predict α decay half-lives of unsynthesized superheavy nuclei.

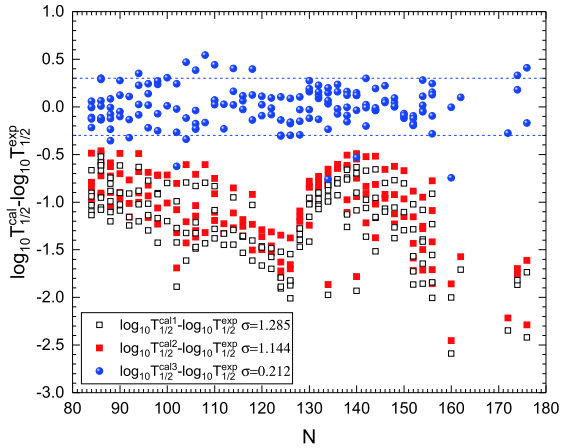

Fig. 2. (color online) The logarithmic differences between three calculated α decay half-lives and experimental data of even-even nuclei. The black open squares, red solid squares, and blue solid circles denote the differences caused by $\lg T_{1/2}^{\rm cal1}$, $\lg T_{1/2}^{\rm cal2}$, and $\lg T_{1/2}^{\rm cal3}$, respectively.

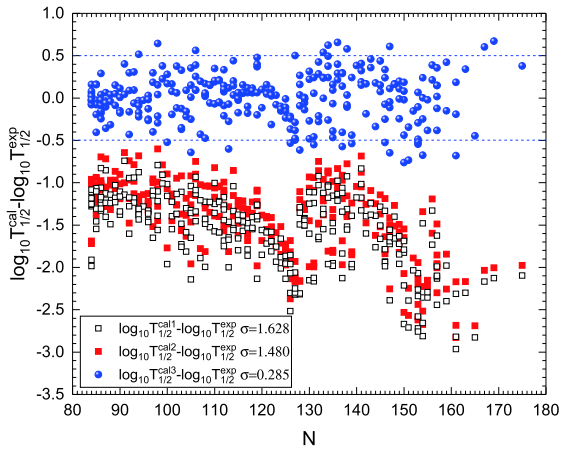

Fig. 3. (color online) Same as Fig. 2, but depicting the logarithmic differences between three calculated α decay half-lives and experimental data of odd-A nuclei.

Encouraged by the good precision of the calculated α decay half-lives for known nuclei, the α decay half-lives of even-even superheavy nuclei with $Z = 112-122$ are predicted using the GLDM with proximity energy Prox. 77-Set 13 and α-particle preformation factors obtained from Eq. (3), the improved Royer formula [79], and the UDL [80]. The α decay energies are taken from the WS4+ mass model [86], which is the most accurate nuclear mass model at present. The predictions are listed in Table 7. In each part of this table, the first, second, and fourth columns are the same as those of Tables 4–6. The third one is the α decay energy obtained by the WS4+ mass model [86]. The last three columns are the predicted α decay half-lives by the improved Royer formula, the UDL formula, and the GLDM with proximity energy Prox. 77-Set 13 and the α-particle preformation factor obtained from Eq. (3). From this table, one can see that the three calculations are consistent with each other, and that the change trends of half-lives are consistent. Additionally, the logarithms of half-lives from the three methods are plotted in Fig. 6. In this figure, one can see that GLDM and UDL formulas give the longest and shortest predictions of α decay half-lives, respectively. The predictions by the GLDM are very close to the ones predicted by the improved Royer formula. Notably, for ^{286}Fl, ^{288}Fl, ^{290}Lv, ^{292}Lv, and ^{294}Og, the predictions can reproduce experimental data well, indicating that the predictions are reliable. In particular, one can find that when neutron numbers N cross $N = 184$, the predicted α decay half-lives decrease sharply, and at $N = 186$, the α decay half-lives reduce by more than two orders of magnitude. It is indicated that strong shell effects are reflected, implying that the next neutron magic number after $N = 126$ is $N = 184$. Fig. 7 shows plots of the logarithms of half-

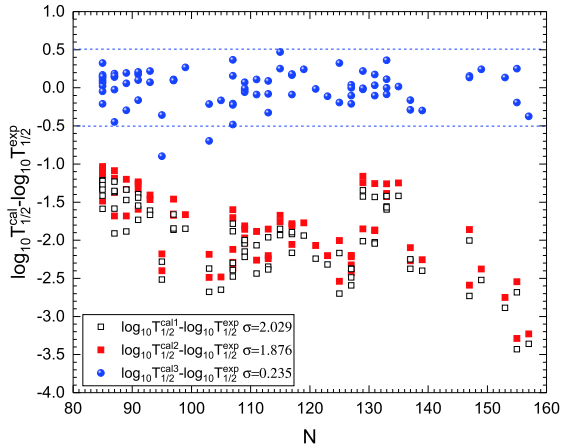

Fig. 4. (color online) Same as Fig. 2, but depicting the logarithmic differences between three calculated α decay half-lives and experimental data of doubly odd nuclei.

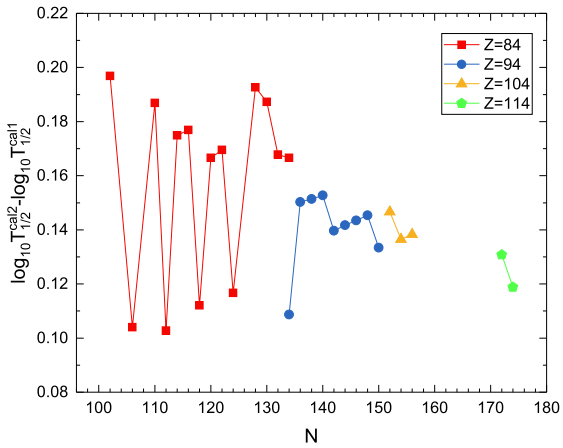

Fig. 5. (color online) The differences between calculated α decay half-lives $\lg T_{1/2}^{\rm cal2}$ and $\lg T_{1/2}^{\rm cal1}$ for even-even nuclei with $Z = 84$, 94, 104, and 114.

Table 7. Predicted α decay half-lives of even-even nuclei with $Z = 112-122$ using the GLDM with proximity energy Prox. 77-Set 13, the improved Royer formula [79], and the universal decay law [80]. The α decay energies are calculated by the WS4+ mass model [86]. The α decay energies and half-lives are in units of MeV and s, respectively.

α transition		Q_α	$l_{\min}$	$\lg T_{1/2}^{\rm Royer}$	$\lg T_{1/2}^{\rm UDL}$	$\lg T_{1/2}^{\rm calc3}$	α transition		Q_α	$l_{\min}$	$\lg T_{1/2}^{\rm Royer}$	$\lg T_{1/2}^{\rm UDL}$	$\lg T_{1/2}^{\rm calc3}$
						Nucsth $Z = 112$							
^{272}Cn	^{268}Ds	12.05	0	−5.32	−5.62	−5.04	^{274}Cn	^{270}Ds	11.52	0	−4.18	−4.5	−4.04
^{276}Cn	^{272}Ds	11.9	0	−5.08	−5.38	−4.85	^{278}Cn	^{274}Ds	11.74	0	−4.75	−5.06	−4.52
^{280}Cn	^{276}Ds	10.83	0	−2.63	−2.96	−2.53	^{282}Cn	^{278}Ds	10.11	0	−0.76	−1.11	−0.69
^{284}Cn	^{280}Ds	9.52	0	0.94	0.57	0.97	^{286}Cn	^{282}Ds	9.01	0	2.51	2.13	2.53
^{288}Cn	^{284}Ds	9.09	0	2.24	1.86	2.27	^{290}Cn	^{286}Ds	8.85	0	2.98	2.59	3.01
^{292}Cn	^{288}Ds	8.27	0	5.06	4.65	5.08	^{294}Cn	^{290}Ds	8.06	0	5.83	5.41	5.81
^{296}Cn	^{292}Ds	7.7	0	7.24	6.81	7.21	^{298}Cn	^{294}Ds	8.77	0	3.12	2.73	3.18
^{300}Cn	^{296}Ds	8.42	0	4.36	3.96	4.42	^{302}Cn	^{298}Ds	7.49	0	8.05	7.61	8.08
						Nuclei with $Z = 114$							
^{274}Fl	^{270}Cn	12.95	0	−6.58	−6.91	−6.21	^{276}Fl	^{272}Cn	12.41	0	−5.5	−5.84	−5.22
^{278}Fl	^{274}Cn	12.51	0	−5.75	−6.09	−5.43	^{280}Fl	^{276}Cn	12.19	0	−5.11	−5.45	−4.84
^{282}Fl	^{278}Cn	11.34	0	−3.23	−3.59	−3.08	^{284}Fl	^{280}Cn	10.54	0	−1.24	−1.62	−1.19
^{286}Fl	^{282}Cn	9.94	0	0.4	−0.002	0.45	^{288}Fl	^{284}Cn	9.62	0	1.33	0.92	1.35
^{290}Fl	^{286}Cn	9.5	0	1.68	1.26	1.71	^{292}Fl	^{288}Cn	8.93	0	3.49	3.06	3.52
^{294}Fl	^{290}Cn	8.69	0	4.3	3.86	4.29	^{296}Fl	^{292}Cn	8.54	0	4.81	4.37	4.8
^{298}Fl	^{294}Cn	8.25	0	5.87	5.41	5.87	^{300}Fl	^{296}Cn	9.54	0	1.37	0.97	1.48
^{302}Fl	^{298}Cn	9.27	0	2.19	1.78	2.31	^{304}Fl	^{300}Cn	8.41	0	5.15	4.71	5.17
						Nuclei with $Z = 116$							
^{276}Lv	^{272}Fl	13.43	0	−6.92	−7.28	−6.47	^{278}Lv	^{274}Fl	12.99	0	−6.09	−6.47	−5.71
^{280}Lv	^{276}Fl	12.94	0	−6.03	−6.4	−5.66	^{282}Lv	^{278}Fl	12.35	0	−4.84	−5.23	−4.58
^{284}Lv	^{280}Fl	11.8	0	−3.67	−4.06	−3.52	^{286}Lv	^{282}Fl	11.28	0	−2.47	−2.88	−2.36
^{288}Lv	^{284}Fl	11.26	0	−2.45	−2.86	−2.36	^{290}Lv	^{286}Fl	11.06	0	−1.98	−2.4	−1.89
^{292}Lv	^{288}Fl	11.1	0	−2.13	−2.54	−2.01	^{294}Lv	^{290}Fl	10.64	0	−0.97	−1.39	−0.88
^{296}Lv	^{292}Fl	10.87	0	−1.61	−2.02	−1.51	^{298}Lv	^{294}Fl	10.75	0	−1.33	−1.74	−1.22
^{300}Lv	^{296}Fl	10.9	0	−1.76	−2.16	−1.61	^{302}Lv	^{298}Fl	12.17	0	−4.81	−5.18	−4.49
^{304}Lv	^{300}Fl	11.45	0	−3.19	−3.58	−3	^{306}Lv	^{302}Fl	10.29	0	−0.2	−0.62	−0.07
						Nuclei with $Z = 118$							
^{278}Og	^{274}Lv	13.93	0	−7.28	−7.69	−6.74	^{280}Og	^{276}Lv	13.73	0	−6.95	−7.35	−6.45
^{282}Og	^{278}Lv	13.49	0	−6.54	−6.95	−6.07	^{284}Og	^{280}Lv	13.21	0	−6.02	−6.44	−5.66
^{286}Og	^{282}Lv	12.89	0	−5.42	−5.84	−5.1	^{288}Og	^{284}Lv	12.59	0	−4.83	−5.25	−4.57
^{290}Og	^{286}Lv	12.57	0	−4.83	−5.25	−4.56	^{292}Og	^{288}Lv	12.21	0	−4.08	−4.51	−3.84
^{294}Og	^{290}Lv	12.17	0	−4.03	−4.46	−3.82	^{296}Og	^{292}Lv	11.73	0	−3.04	−3.48	−2.91
^{298}Og	^{294}Lv	12.16	0	−4.07	−4.5	−3.86	^{300}Og	^{296}Lv	11.93	0	−3.59	−4.02	−3.38
^{302}Og	^{298}Lv	12.02	0	−3.83	−4.25	−3.59	^{304}Og	^{300}Lv	13.1	0	−6.17	−6.57	−5.77
^{306}Og	^{302}Lv	12.46	0	−4.87	−5.28	−4.59	^{308}Og	^{304}Lv	11.18	0	−1.93	−2.37	−1.77
						Nuclei with $Z = 120$							
^{284}120	^{280}Og	13.99	0	−6.91	−7.35	−6.44	^{286}120	^{282}Og	14.01	0	−6.99	−7.43	−6.46
^{288}120	^{284}Og	13.71	0	−6.45	−6.9	−6.01	^{290}120	^{286}Og	13.68	0	−6.43	−6.88	−5.97
^{292}120	^{288}Og	13.44	0	−6.01	−6.46	−5.57	^{294}120	^{290}Og	13.22	0	−5.6	−6.05	−5.25

Continued on next page

Table 7-continued from previous page

α transition		Q_α	$l_{\min}$	$\lg T_{1/2}^{\rm Royer}$	$\lg T_{1/2}^{\rm UDL}$	$\lg T_{1/2}^{\rm calc3}$	α transition		Q_α	$l_{\min}$	$\lg T_{1/2}^{\rm Royer}$	$\lg T_{1/2}^{\rm UDL}$	$\lg T_{1/2}^{\rm calc3}$
^{296}120	^{292}Og	13.32	0	−5.84	−6.29	−5.46	^{298}120	^{294}Og	12.98	0	−5.2	−5.65	−4.87
^{300}120	^{296}Og	13.29	0	−5.87	−6.31	−5.45	^{302}120	^{298}Og	12.87	0	−5.03	−5.48	−4.67
^{304}120	^{300}Og	12.74	0	−4.8	−5.25	−4.53	^{306}120	^{302}Og	13.77	0	−6.88	−7.31	−6.38
^{308}120	^{304}Og	12.95	0	−5.3	−5.75	−4.95	^{310}120	^{306}Og	11.48	0	−2.01	−2.49	−1.86
Nuclei with Z = 122													
^{290}122	^{286}120	15.09	0	−8.37	−8.84	−7.62	^{292}122	^{288}120	14.99	0	−8.24	−8.71	−7.48
^{294}122	^{290}120	14.64	0	−7.68	−8.15	−7.05	^{296}122	^{292}120	14.67	0	−7.76	−8.23	−7.14
^{298}122	^{294}120	14.68	0	−7.81	−8.28	−7.17	^{300}122	^{296}120	14.2	0	−6.99	−7.46	−6.42
^{302}122	^{298}120	14.21	0	−7.05	−7.52	−6.46	^{304}122	^{300}120	13.71	0	−6.15	−6.63	−5.73
^{306}122	^{302}120	13.78	0	−6.31	−6.79	−5.87	^{308}122	^{304}120	14.92	0	−8.4	−8.86	−7.64
^{310}122	^{306}120	13.44	0	−5.71	−6.19	−5.28	^{312}122	^{308}120	12.14	0	−2.97	−3.48	−2.75

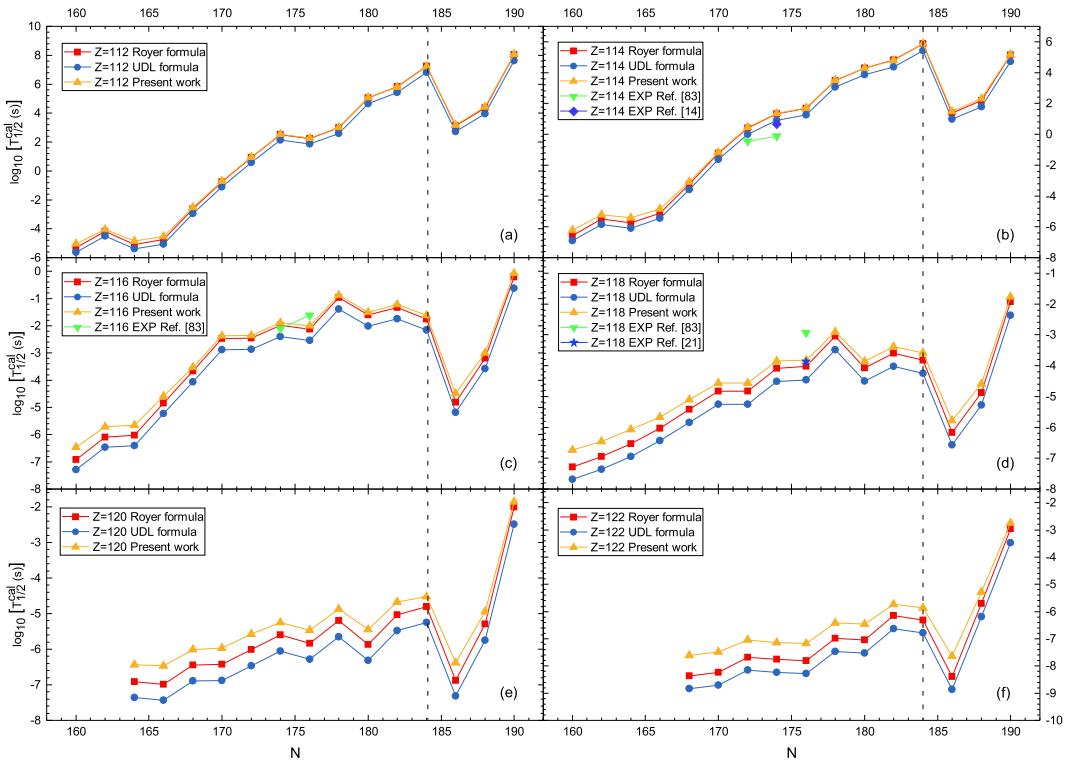

Fig. 6. (color online) The predicted α decay half-lives of even-even nuclei with $Z = 112-122$ using the GLDM with proximity energy Prox. 77-Set 13 and α-particle preformation factors obtained from Eq. (3), the improved Royer formula [79], and the universal decay law [80], taking Q_α obtained from the WS4+ mass model [86]. The purple square, blue star, and green triangles denote the experimental α decay half-lives taken from Refs. [14, 21, 83].

lives for the three methods for $N = 184$ isotones. In this figure, one can see that when the proton number $Z > 114$, the predicted α decay half-lives drop dramatically by eight orders of magnitude at $Z = 116$, indicating that there is a major proton shell, and the next proton magic number after $Z = 82$ is $Z = 114$. In addition, the half-life of ^{296}Og shows a peak, where the nucleus is the closest one to the heaviest nucleus ^{295}Og at present and may be the next candidate for synthesizing a superheavy nucleus.

IV. SUMMARY

In summary, we systematically studied the abilities of various versions of proximity energies when they are applied to the GLDM for enhancing the calculation accur-

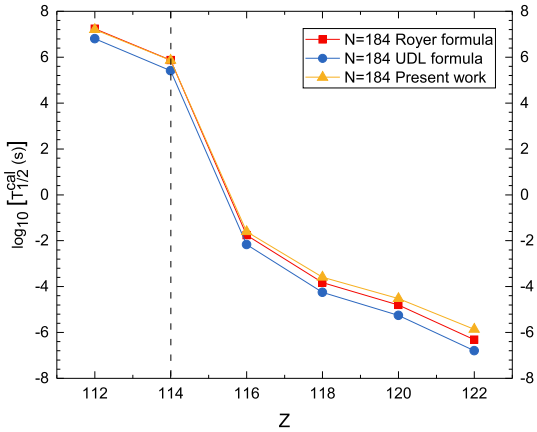

Fig. 7. (color online) Same as Fig. 6, but depicting predicted α decay half-lives of even-even nuclei with N = 184 isotones.

acy and prediction ability of α decay half-lives for known and unsynthesized superheavy nuclei. When a more suitable proximity energy is chosen for application to the GLDM, calculations of α half-lives exhibit systematic improvements in reproducing experimental data. In addition, the calculations indicate that changing the proximity energy will not affect the revealing of the microscopic shell effect, which is important for predicting the island of stability for superheavy nuclei. Encouraged by this, the α decay half-lives of even-even superheavy nuclei with $Z = 112-122$ were predicted by the GLDM with a more suitable proximity energy. The predictions conform to the ones calculated by the improved Royer formula and the UDL. In addition, the features of the predicted α decay half-lives imply that the next double magic nucleus after ^{208}Pb is ^{298}Fl.

References

[1] S. Hofmann and G. Münzenberg, Rev. Mod. Phys. **72**, 733-767 (2000)
[2] M. Pfützner, M. Karny, L. V. Grigorenko, and K. Riisager, Rev. Mod. Phys. **84**, 567-619 (2012)
[3] A. N. Andreyev, M. Huyse, P. Van Duppen, *et al.*, Phys. Rev. Lett. **110**, 242502 (2013)
[4] L. Ma, Z. Y. Zhang, Z. G. Gan *et al.*, Phys. Rev. C **91**, 051302(R) (2015)
[5] W. M. Seif, Phys. Rev. C **74**, 034302 (2006)
[6] J. Khuyagbaatar, A. Yakushev, Ch. E. Düllmann *et al.*, Phys. Rev. Lett. **112**, 172501 (2014)
[7] R. J. Carroll, R. D. Page, D. T. Joss *et al.*, Phys. Rev. Lett. **112**, 092501 (2014)
[8] D. S. Delion, R. J. Liotta, and R. Wyss, Phys. Rev. C **92**, 051301(R) (2015)
[9] W. M. Seif, M. Shalaby, and M. F. Alrakshy, Phys. Rev. C **84**, 064608 (2011)
[10] Y. Ren and Z. Ren, Phys. Rev. C **85**, 044608 (2012)
[11] Y. Qian, Z. Ren, and D. Ni, Phys. Rev. C **89**, 024318 (2014)
[12] Z. Ren, Phys. Rev. C **65**, 051304(R) (2002)
[13] M. Brack, J. Damgaard, A. S. Jensen *et al.*, Rev. Mod. Phys. **44**, 320-405 (1972)
[14] Yu. Ts. Oganessian, V. K. Utyonkov, Yu. V. Lobanov *et al.*, Phys. Rev. C **63**, 011301(R) (2000)
[15] Yu. Ts. Oganessian, V. K. Utyonkov, Yu. V. Lobanov *et al.*, Phys. Rev. C **76**, 011601(R) (2007)
[16] P. A. Ellison, K. E. Gregorich, J. S. Berryman *et al.*, Phys. Rev. Lett. **105**, 182701 (2010)
[17] Yu. Ts. Oganessian, F. Sh. Abdullin, P. D. Bailey *et al.*, Phys. Rev. Lett. **104**, 142502 (2010)
[18] J. H. Hamilton., S. Hofmann, and Y. T. Oganessian, Ann. Rev. Nucl. Part. Sci. **63**(1), 383-405 (2013)
[19] Kosuke Morita, Kouji Morimoto, Daiya Kaji *et al.*, J. Phys. Soc. Jpn. **76**(4), 045001-045001 (2007)
[20] Y. T. Oganessian, Radiochim. Acta **99**, 429-439 (2011)
[21] Yu. Ts. Oganessian, F. Sh. Abdullin, C. Alexander *et al.*, Phys. Rev. Lett. **109**, 162501 (2012)
[22] H. F. Zhang and G. Royer, Phys. Rev. C **77**, 054318 (2008)
[23] K. P. Santhosh, J. G. Joseph, and S. Sahadevan, Phys. Rev. C **82**, 064605 (2010)
[24] K. P. Santhosh and J. G. Joseph, Phys. Rev. C **86**, 024613 (2012)
[25] K. P. Santhosh, B. Priyanka, and M. S. Unnikrishnan, Phys. Rev. C **85**, 034604 (2012)
[26] J.-G. Deng, J.-C. Zhao, P.-C. Chu *et al.*, Phys. Rev. C **97**, 044322 (2018)
[27] J.-G. Deng, J.-C. Zhao, D. Xiang *et al.*, Phys. Rev. C **96**, 024318 (2017)
[28] J.-G. Deng, J.-H. Cheng, B. Zheng *et al.*, Chin. Phys. C **41**(12), 124109 (2017)
[29] J.-G. Deng, J.-C. Zhao, J.-L. Chen *et al.*, Chin. Phys. C **42**(4), 044102 (2018)
[30] C. Xu and Z. Ren, Nucl. Phys. A **760**(3), 303-316 (2005)
[31] C. Xu and Z. Ren, Phys. Rev. C **74**, 014304 (2006)
[32] C. Xu and Z. Ren, Phys. Rev. C **73**, 041301(R) (2006)
[33] Y. Qian and Z. Ren, Nucl. Phys. A **852**(1), 82-91 (2011)
[34] Y. Qian and Z. Ren, Phys. Rev. C **85**, 027306 (2012)
[35] W. M. Seif, Phys. Rev. C **91**, 014322 (2015)
[36] W. M. Seif, M. M. Botros, and A. I. Refaie, Phys. Rev. C **92**, 044302 (2015)
[37] G Royer, J. Phys. G **26**(8), 1149-1170 (2000)
[38] Y. Z. Wang, J. M. Dong, B. B. Peng *et al.*, Phys. Rev. C **81**, 067301 (2010)
[39] H. Zhang, H. Zhang, J. Li, X. Bao *et al.*, Phys. Rev. C **90**, 054313 (2014)
[40] X. Bao, H. Zhang, H. Zhang *et al.*, Nucl. Phys. A **921**, 85-95 (2014)
[41] J. M. Dong, H. F. Zhang, and G. Royer, Phys. Rev. C **79**, 054330 (2009)
[42] X. J. Bao, H. F. Zhang, B. S. Hu *et al.*, J. Phys. G **39**(9), 095103 (2012)
[43] G. Royer and B. Remaud, Nucl. Phys. A **444**(3), 477-497 (1985)
[44] G. Royer and K. Zbiri, Nucl. Phys. A **697**(3), 630-638 (2002)
[45] H. Zhang, W. Zuo, J. Li *et al.*, Phys. Rev. C **74**, 017304 (2006)
[46] H. F. Zhang and G. Royer, Phys. Rev. C **76**, 047304 (2007)
[47] G. Royer and H. F. Zhang, Phys. Rev. C **77**, 037602 (2008)
[48] Y. Z. Wang, H. F. Zhang, J. M. Dong *et al.*, Phys. Rev. C **79**, 014316 (2009)
[49] J. Blocki, J. Randrup, W. J. Świątecki *et al.*, Ann. Phys. (NY) **105**(2), 427-462 (1977)
[50] Y. J. Yao, G. L. Zhang, W. W. Qu *et al.*, Eur. Phys. J. A

51(9), 122 (2015)
[51] O. N. Ghodsi and A. Daei-Ataollah, Phys. Rev. C **93**, 024612 (2016)
[52] J Blocki and W. J. Świątecki, Ann. Phys. (NY) **132**(1), 53-65 (1981)
[53] I. Dutt and R. K. Puri, Phys. Rev. C **81**, 044615 (2010)
[54] J.-G. Deng, X.-H. Li, J.-L. Chen *et al*., Eur. Phys. J. A **55**(4), 58 (2019)
[55] W. D. Myers and W. J. Świątecki, Nucl. Phys. **81**(1), 1-60 (1966)
[56] P. Möller, Nucl. Phys. A **272**(2), 502-532 (1976)
[57] H. J. Krappe, J. R. Nix, and A. J. Sierk, Phys. Rev. C **20**, 992-1013 (1979)
[58] P. Möller and J. Rayford Nix, Nucl. Phys. A **361**(1), 117-146 (1981)
[59] G Royer and B Remaud, J. Phys. G **10**(8), 1057-1070 (1984)
[60] P. Möller and J.R. Nix, At. Data Nucl. Data Tables **39**(2), 213-223 (1988)
[61] P. Möller, J.R. Nix, W.D. Myers *et al*., At. Data Nucl. Data Tables **59**(2), 185-381 (1995)
[62] K. Pomorski and J. Dudek, Phys. Rev. C **67**, 044316 (2003)
[63] W. D. Myers and W. J. Świątecki, Phys. Rev. C **62**, 044610 (2000)
[64] I. Dutt and R. Bansal, Chin. Phys. Lett. **27**(11), 112402 (2010)
[65] I. Dutt, Pramana **76**(6), 921-931 (2011)
[66] R. Bass, Phys. Lett. B **47**(2), 139-142 (1973)
[67] R. Bass, Nucl. Phys. A **231**(1), 45-63 (1974)
[68] R. Bass, Phys. Rev. Lett. **39**, 265-268 (1977)
[69] W Reisdorf, J. Phys. G **20**(9), 1297 (1994)
[70] P.R. Christensen and A. Winther, Phys. Lett. B **65**(1), 19-22 (1976)
[71] A. Winther, Nucl. Phys. A **594**(2), 203-245 (1995)
[72] H. Ngô and C. Ngô, Nucl. Phys. A **348**(1), 140-156 (1980)
[73] V. Y. Denisov, Phys. Lett. B **526**(3), 315-321 (2002)
[74] C.L. Guo, G.L. Zhang, and X.Y. Le, Nucl. Phys. A **897**, 54-61 (2013)
[75] K. P. Santhosh, C. Nithya, H. Hassanabadi *et al*., Phys. Rev. C **98**, 024625 (2018)
[76] D. T. Akrawy, K. P. Santhosh, and H. Hassanabadi, Phys. Rev. C **100**, 034608 (2019)
[77] K. P. Santhosh, Dashty T. Akrawy, H. Hassanabadi *et al*., Phys. Rev. C **101**, 064610 (2020)
[78] H. C. Manjunatha, N. Sowmya, N. Manjunath *et al*., Int. J. Mod. Phys. E **29**(05), 2050028 (2020)
[79] J.-G. Deng, H.-F. Zhang, and G. Royer, Phys. Rev. C **101**, 034307 (2020)
[80] C. Qi, F. R. Xu, R. J. Liotta *et al*., Phys. Rev. Lett. **103**, 072501 (2009)
[81] J.-G. Deng and H.-F. Zhang, Phys. Rev. C **102**, 044314 (2020)
[82] V. Yu. Denisov and A. A. Khudenko, Phys. Rev. C **79**, 054614 (2009)
[83] G. Audi, F. G. Kondev, M. Wang *et al*., Chin. Phys. C **41**(3), 030001 (2017)
[84] W. J. Huang, G. Audi, M. Wang *et al*., Chin. Phys. C **41**(3), 030002 (2017)
[85] M. Wang, G. Audi, F. G. Kondev *et al*., Chin. Phys. C **41**(3), 030003 (2017)
[86] N. Wang, M. Liu, X. Wu *et al*., Phys. Lett. B **734**, 215 (2014)